

N 70 42369

CR 114117

Title: Laser Technology for Communications

Prepared for

Contract Report to the Office of Naval Research, Arlington, Virginia

CASE FILE
COPY

CASE WESTERN RESERVE UNIVERSITY
Division of Electrical Sciences and Applied Physics
School of Engineering

Semi-Annual Technical Progress Report No. 1
1 February to 31 July, 1970

NASA Grant No. NGR 36-027-014

Title: Laser Technology for Communications

Prepared for

National Aeronautics and Space Administration
Advanced Development Division
Goddard Space Flight Center
Greenbelt, Maryland

Laser Technology for Communications

Semi Annual Report No. 1

Principal Investigator: Yoh-Han Pao, Professor and Head of
The Division of Electrical Sciences
and Applied Physics

Contributors to Program: Robert Yusek, Assistant Professor
Paul C. Claspy, Ph.D. Candidate
Mark W. Goldberg, Ph.D. Candidate
Denis R. Hall, Ph.D. Candidate

TABLE OF CONTENTS

	<u>Page</u>
1. INTRODUCTION	1
2. SUMMARY OF WORK ACCOMPLISHED DURING PERIOD	4
3. STARK MODULATION OF CO ₂ LASERS	6
3.1 Evaluation of Gases	7
3.2 Experimental Arrangement	8
3.3 Experimental Procedure	11
3.4 Intracavity Modulation Results	12
3.5 Modulation Linearity	17
4. COMPETITION BETWEEN TRANSITIONS IN A CO ₂ LASER	23
4.1 The CO ₂ Laser Signature Problem	23
4.2 Apparatus and Experiments	23
4.3 Experimental Results	26
4.4 Discussion of Results	41
5. VERY HIGH RESOLUTION INVERTED LAMB DIP SPECTRA OF SF ₆	42
5.1 Background of Investigation	42
5.2 Apparatus and Experiments	43
5.3 Discussion of Results	49
6. PLANS FOR NEXT SEMI-ANNUAL PERIOD	53
7. REFERENCES	54
8. LIST OF FIGURES	55
9. LIST OF TABLES	58

LASER TECHNOLOGY FOR COMMUNICATIONS

1. INTRODUCTION

This document reports the activities and principal results of the first six months of an innovative program in the development of laser technology for communications. The program consists of a number of basic investigations in those technical areas deemed to be particularly crucial for laser communications. There is also an overall effort aimed at rapid development of the basic results of these in-depth studies.

Of the various efforts reported here, the study of the Stark effect in molecular gases is clearly relevant to the need for wideband modulators for lasers operating at infrared wavelengths. In fact, the Stark effect studies proved to be successful in this respect. It is now clear that Stark field gas modulators are practical and are competitive with electro-optic crystal modulators.

In a second investigation, we studied how a CO₂ laser in a space approved laser package would perform as the gas pressure decreased with age, as the discharge current varied, as the cavity length changed and/or as the electro-optic crystal modulator heated up perhaps unevenly in the cavity. Since the various transitions in the 9.6 μ and 10.6 μ wavelength regions compete with each other, initially it was quite questionable whether a CO₂ laser operating

without any frequency selecting element in the cavity could always be depended upon to oscillate at some specifically chosen transition even if the cavity length could be tuned at will. This problem was named the "CO₂ laser signature problem". A stable laser was specifically built for this investigation and an extensive series of experiments showed that quite fortunately certain lines always oscillated and could be depended upon to compete effectively with all other transitions over a wide range of operating conditions.

The third investigation carried out during this past six month period concerns laser stabilization schemes and the realization of tunable local oscillators. The actual investigation was in the form of a high resolution and high sensitivity investigation of the molecular spectra of the gas SF₆ in the 10.6μ micron wavelength region. The technique used is a novel combination of heterodyne detection and Inverted Lamb Dip Spectroscopy.

The principal features of the results of these three investigations are summarized in section 2. The details of these investigations are presented in sections 3, 4 and 5.

An account of the CO₂ laser signature problem has been accepted for publication in Applied Optics. The Inverted Lamb Dip Spectra of SF₆ is being prepared for publication probably in Applied Physics Letters.

At present there are no immediate plans for publication of the Stark Modulation results. However accounts of some facets of this work will be presented at the UMR-Kelly Communications Conference to be held in October 1970 at the University of Missouri and also at the October meeting of the Optical Society of America. It is expected that Paul C. Claspy's thesis on High Frequency Stark Modulation of CO₂ Lasers will be submitted for publication on completion.

2. SUMMARY OF WORK ACCOMPLISHED DURING PERIOD

In the Stark modulation studies, seventeen gases were evaluated as possible candidates for use in gas modulators for CO₂ lasers. In so far as linearity of response to the Stark field, depth of modulation and lack of dispersion with respect to frequency, the most promising gas and laser line combinations are 1,1 Difluoroethylene with the P(22) line of the 10.6 μ transition and Methyl bromide with the P(26) line of the 9.6 μ transition.

For these combinations and for out of cavity modulators, a 50% modulation can be obtained with a modulator about 50 cm long and an applied field of 400 volts peak to peak and a 400 v/cm D.C. bias field. It was demonstrated that a five path cell 10 cms in length would perform equally well. At a gas pressure of about 1.5 Torr, the response did not change with frequency up to 25 MHz. It is expected that such nondispersive response may be obtained to about 80 MHz, above which dispersion becomes noticeable and the magnitude of the response decreases with frequency.

In the 'CO₂ laser signature problem' investigation, it was found that it is possible to operate a CO₂ laser without a frequency selecting unit in the cavity and confidently expect that the 10.6 μ lines P(16), P(18) and P(20) will oscillate provided the cavity length can be tuned over a distance of about 5 microns. These

transitions dominate so effectively over other transitions, that they oscillate over quite a large portion of their normal gain curve even in the face of such competition. This dominance is sustained over a large range of laser operating conditions.

The Inverted Lamb Dip method of studying the details of molecular spectra is very powerful because the method effectively strips an absorption line of its inhomogeneous broadening and reveals whether an apparently broad line is really made up of several overlapping independent transitions. Using heterodyne detection in combination with Inverted Lamb Dip spectroscopy has so increased the accuracy of the method that minute details of the absorption spectra of SF₆ in the spectral regions of the P(16), and P(18) lines of the 00⁰₁ - 10⁰₀ transition of the CO₂ laser have now been revealed. It turns out that there are 24 lines within the gain curve of the P(16) line of the 00⁰₁ - 10⁰₀ transition and it was possible to observe 43 SF₆ absorption lines within the gain curve of the P(18) line of the same 10.6μ transition. Using heterodyne methods, line spacings on the order of 1 MHz were measured and the resulting line spectra were referenced to lasing line center.

3. STARK MODULATION OF CO₂ LASERS

Although a great deal is known about Stark effects in electronic and microwave spectra, until recently there has been very little interest in the effects of Stark fields on vibrational-rotational infrared spectra of molecular gases.

Landman and Morantz¹ were first to demonstrate that the Stark effect in molecular gases could be used to modulate the output of infrared lasers. Their preliminary work was carried out at frequencies not exceeding 256 Hertz and involved the use of high modulating fields typically of the order of 1 kilovolt/cm or more. Since then Claspy and Pao^{2,3} have extended these techniques to high frequencies and have also exploited the use of D.C. bias fields to circumvent the use of high modulating A.C. fields.

The purpose of the investigations reported here has been to determine which gases are suitable for use as Stark modulators of the carbon dioxide laser. There are several reasons which justify this effort. There exists a real need for an efficient wideband modulator for the intense lines P(16) to P(22) of the 00⁰1 - 10⁰0 bands in CO₂, which are the best candidates as carriers in an optical communications system. A suitable gas which exhibits a large Stark effect on one of these lines would have several advantages over current electro-optic modulators. The gas modulators

operate at relatively low voltages and so require very little power. In addition, these devices are easily constructed and are optically uniform. To further develop Stark effect optical modulators there is need to investigate the effects of electric fields on different molecules when these are subject to intense beams of electromagnetic radiation, to experimentally determine the variation of the Stark effect with light intensity, field intensity and frequency.

3.1 Evaluation of Gases

While, initially some time was spent on the possibility of predicting which gases would be suitable, it was quickly realized that with the spectroscopic data and molecular constants which are currently available, one could make only slightly better than an educated guess as to the usefulness of a particular gas.

On this premise then, the prime consideration in the choice of gases to be evaluated experimentally was the very pragmatic one of availability. The contents of the catalogues of the major gas supply houses were scanned for gases which satisfied the following criteria.

1. The molecular symmetry was either that of a symmetric top or of an asymmetric top,
2. the existence of a permanent dipole moment, and

3. the presence of absorption in the $9.6 \sim 11\mu$ wavelength region.

3.2 Experimental Arrangement

The apparatus used in the evaluation of these gases is shown schematically in Figure 3.1.

The laser system employed a 80 cm laser tube which was water jacketed and had nickel electrodes and sodium chloride windows. The bore of the discharge tube was 7mm and the cavity length 1.69 meters. The laser gas mix was 60.9% He: 16.9% CO₂: 7.5% N₂: 4.65% H₂ and the tube was operated sealed off at one of several pressures between 8 and 16 Torr.

Several different Stark cells have been employed both inside and outside the laser cavity. Most of the work aimed at investigating intracavity modulation was performed with a 10 cm long cell with a 1 cm electrode separation as shown in Figure 3.2. The cell windows (not shown) are 2 inch diameter sodium chloride flats. In addition to the 10 cm cell, another cell of the same type, but 1 meter in length, was used in extra-cavity studies. A third Stark cell of different design was used to explore the effect of variation of the angle between the applied electric field and the polarization of the laser light. This cell consisted of a 32 cm glass tube having 5 mm diameter, which is closed by 1 inch

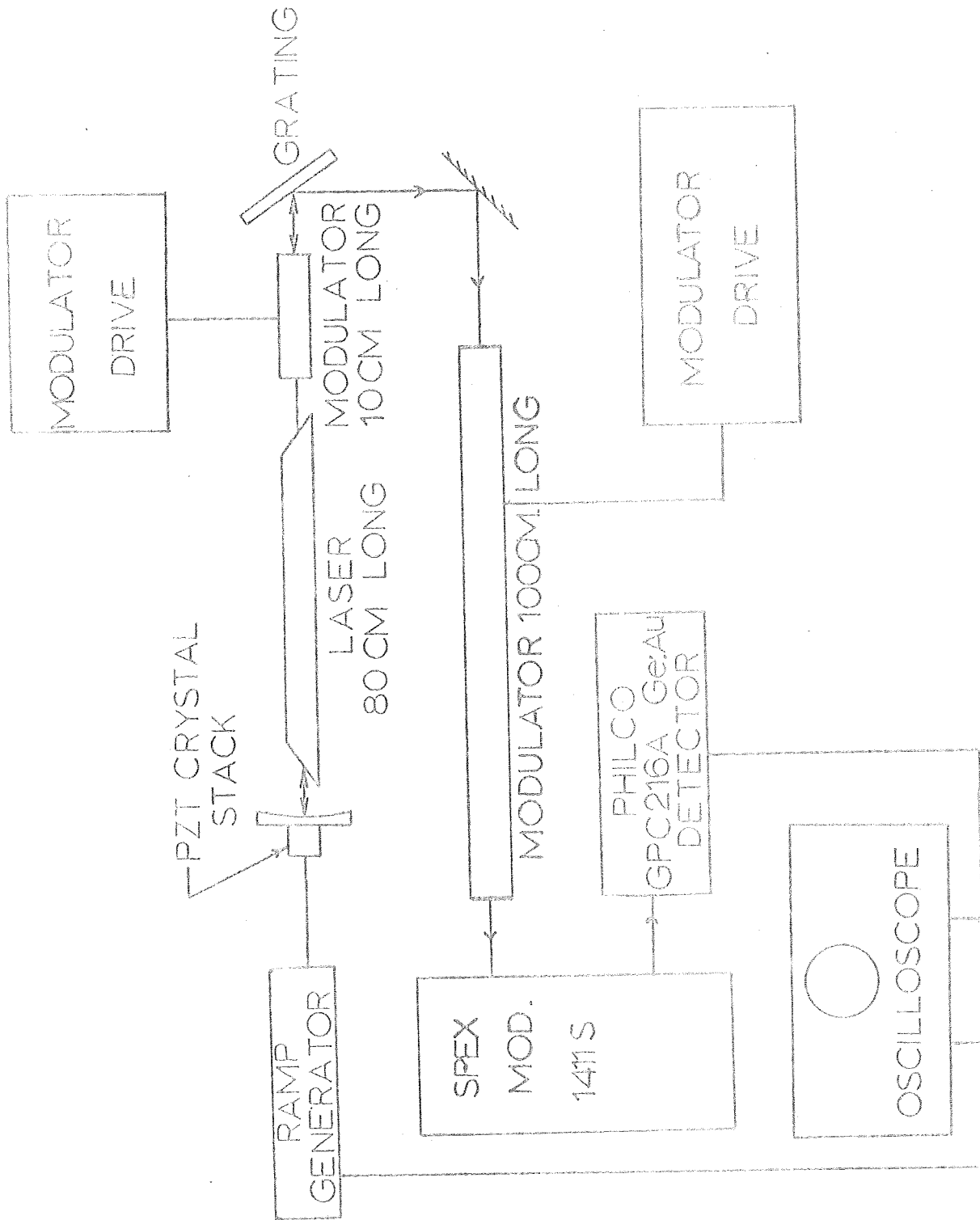


Figure 5.1 Experimental Apparatus for Stark Modulation.

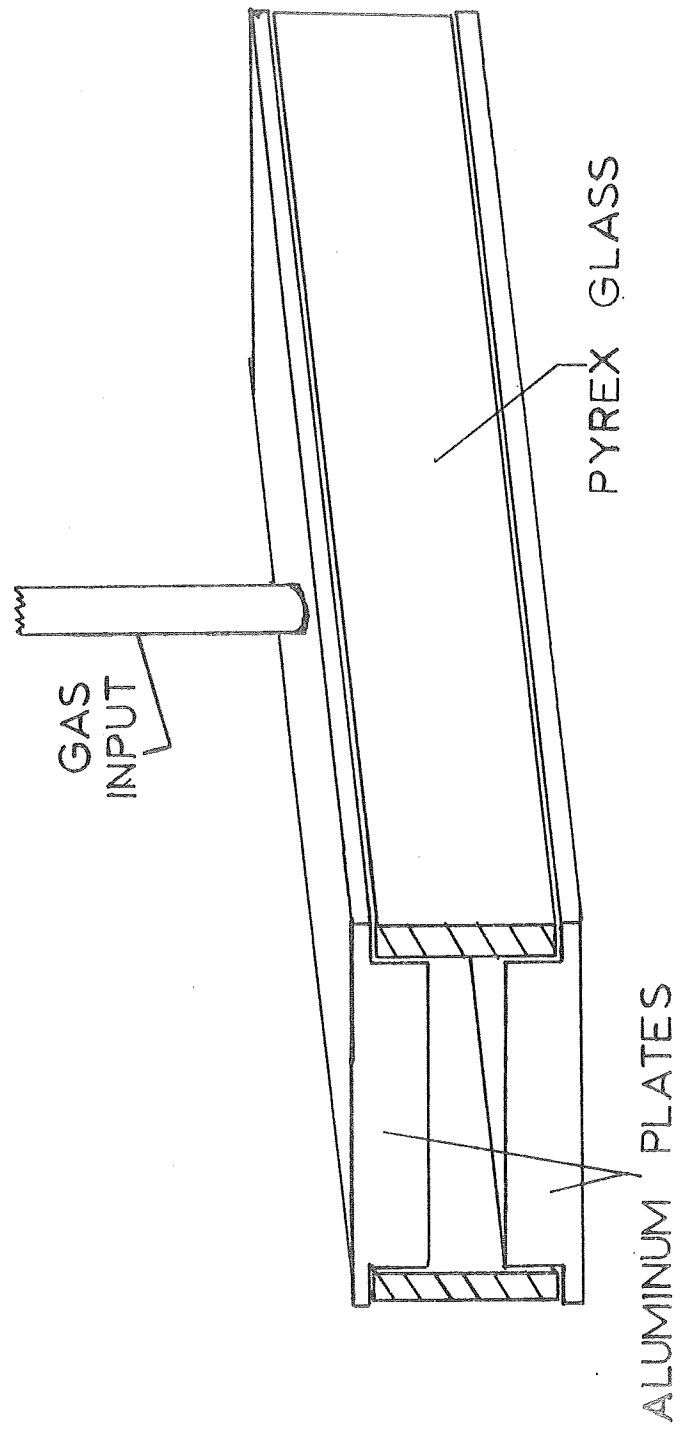


Figure 3.2 Stark Modulator.

NaCl windows. A pair of parallel electrodes, 27 x 4.4 cm, are supported on either side of the gas tube. These plates, which are separated by 7 mm, can be rotated about the tube axis to change the direction of the Stark field.

During these measurements, most of the data were taken at either 32 or 143 KHz. The availability of high voltage oscillators, each capable of up to 1 kv peak to peak output, dictated the choice of these frequencies. A D.C. bias of up to 400 volts could be simultaneously applied to the cell.

3.1.2 Experimental Procedure

The initial investigations on all gases were carried out using the 10 cm Stark cell positioned inside the laser cavity. With the Stark cell evacuated, the laser is first tuned to the line to be studied by adjustment of the cavity reflection grating. The laser gain profile of the selected transition can then be displayed on an oscilloscope by length tuning the cavity with a piezoelectric mirror translator. A sample of the prospective modulator gas is slowly admitted to the intracavity cell. Generally, it was found that gases which subsequently proved to be suitable Stark effect modulators quenched laser oscillation at absorber pressures less than 10 Torr. If this occurred, the absorber was slowly pumped out until laser action just began. At this point, a combination of A.C. and D.C. electric fields were applied to the cell.

Modulation of the laser output could then be observed as time variations of the laser gain profile, as shown in Figure 3.3. The effects of various combinations of A.C. and D.C. field amplitudes were examined at a series of pressures as the cell was further evacuated.

Since the object of these preliminary investigations was to seek gasses which produce large modulation depths on the stronger CO₂ laser lines, and in the interest of examining many gasses quickly, only very rough estimates of modulation depth were made.

3.3 Intracavity Modulation Results

Intracavity Stark modulation has been investigated on the stronger transitions of the 00⁰1 - 10⁰0 band of CO₂ and some lines of the 00⁰1 - 02⁰0 band with the following gasses:

Methyl Chloride	CH ₃ -Cl
Methyl Fluoride	CH ₃ -F
Methyl Bromide	CH ₃ -Br
Vinyl Chloride	C ₂ H ₃ Cl
Vinyl Bromide	C ₂ H ₃ Br
Vinyl Fluoride	C ₂ H ₃ F
Methyl Acetylene	C ₃ H ₄
Ethyl Bromide	C ₂ H ₅ Br
Ethyl Iodide	C ₂ H ₅ I
Dimethyl Ether	(CH ₃) ₂ O
1-1 Difluoroethylene	CH ₂ -CF ₂

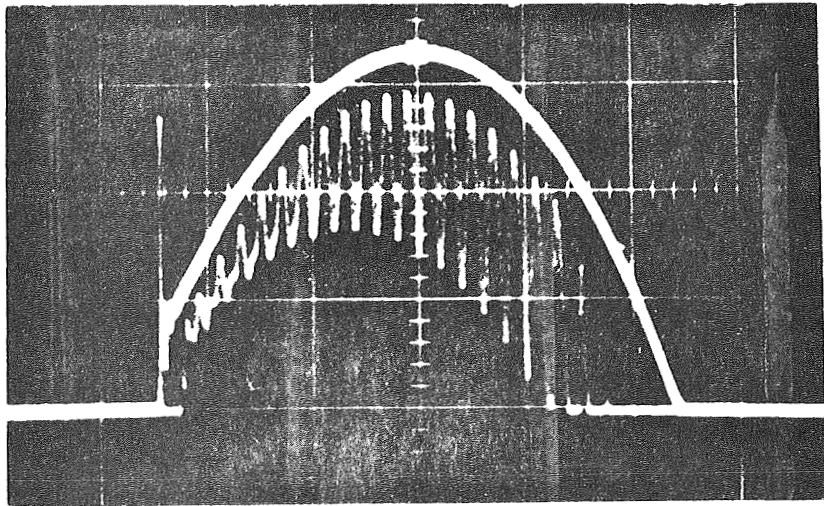


Figure 3.3 Typical Response During Simultaneous Modulation and Laser Sweep.

1-1 Difluoroethane	$\text{CH}_3 - \text{CHF}_2$
Trichloroethylene	$\text{CCl}_2 - \text{CClH}$
Dichlorodifluoromethane	CCl_2F_2
Monochloropentafluoroethane	C_2ClF_5
Propylene	C_3H_6
Bromotrifluoromethane	CF_3Br

Special emphasis was given to the modulation of the P(16) through P(22) lines in the 10.6μ band of CO_2 . These results are presented in Table 3.1. In addition, intracavity modulation has been observed on the following additional gasses and lines indicated. All line designations refer to the $10^00 - 00^01$ band of CO_2 , and underlining signifies large modulation depth. As before, an asterisk denotes passive Q switching.

Vinyl Chloride: P(14)*, R(18), R(20)*, R(22)

Propylene: R(24), R(26)*

1-1 Difluoroethylene: P(10), P(12), P(14), P(24), P(26)
P(28), R(10), R(12), R(14), R(16),
R(18), R(20), R(22), R(26), R(28),
R(30).

1-1 Difluoroethane: P(10), P(12), P(14), P(24), P(26).

Propylene: R(18), R(24), R(26)*.

Methyl Chloride: R(16), R(18), R(20), R(22), R(24).

The many absorption/emission coincidences seen with 1-1 Difluoroethylene and 1-1 difluoroethane warranted further examination of

Table 3.1 Molecular Gasses Suitable for Intracavity
Stark Modulation of the Stronger CO₂ Laser Lines

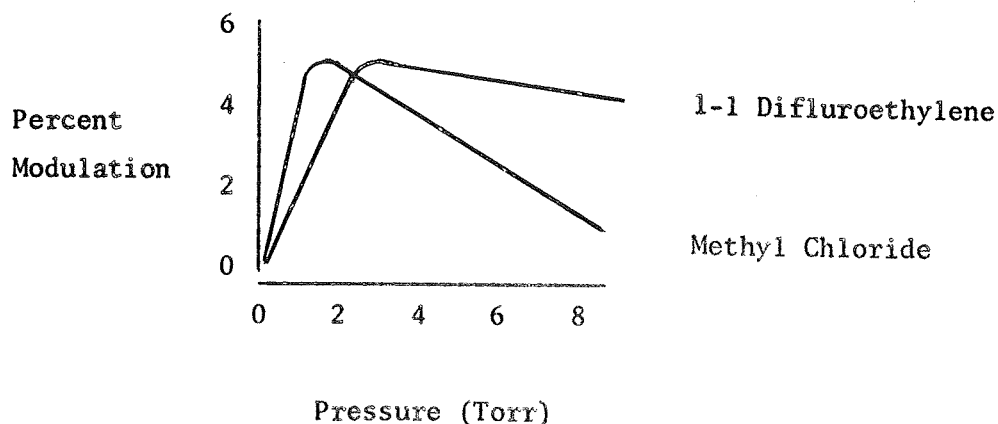
<u>Gas</u>	Modulation of 10.6 μ Laser Transition:			
	<u>P(16)</u>	<u>P(18)</u>	<u>P(20)</u>	<u>P(22)</u>
Vinyl Chloride*	20%	15%	40%	25%
Propylene	small	_____	_____	_____
1-1 Difluoromethylene	30%	15%	100%	100%
1-1 Difluoroethane	30%	70%	100%	80%
Trichloroethylene*	_____	_____	_____	_____
Vinyl Chloride	10%	10%	10%	10%
Bromotrifluoromethane	10%	10%	100%	90%
Dimethyl Ether	Very small	_____	Very small	_____

Note: Gasses marked with an asterisk showed passive
Q switching at higher cell pressures.

these gases as potential Stark effect modulators. Continuing research has emphasized extra-cavity modulators, since these avoid the high frequency cutoff imposed by laser cavity ringing time.

3.4 Out of Cavity Modulation Results for the 1-1 Difluoroethylene/ P(22) Line Combination.

This gas appears the most promising at present for modulation of one of the high gain CO_2 lines. The modulation depth as a function of pressure is quite different from that for other gases, in that the decrease in modulation depth with pressure is much less than that observed with methyl chloride on P(26) of the 9.6μ band of CO_2 .



The above data are for a 30 cm modulator with 218 v/cm A.C. field and 340 v/cm D.C. bias. The response is linear up to this A.C. field.

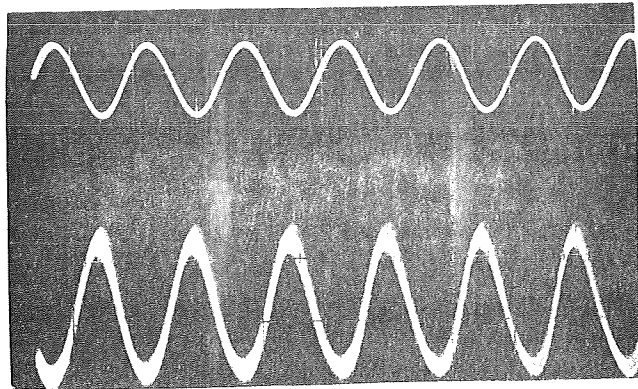
3.5 Modulator Linearity

Operationally, the Stark effect modulator is a voltage-tuned narrow band optical absorber. Loss modulation of a single frequency laser can be accomplished by varying the center frequency of the absorption through the molecular Stark effect. If significant modulation is to occur, then the D.C. Stark field and laser emission frequency must be selected so that laser oscillation falls on a high slope region of the absorption profile. Having chosen such an operating point, one may then expand the absorber lineshape about this point in a power series. Examination of the various terms in the usual manner leads directly to predictions of harmonic distortion whenever the A.C. Stark field intensity becomes large. It must be remembered that the ratios of series coefficients in such an expansion will depend upon the degree of curvature around the operating point. In terms of the experiment at hand, this means that the ratio of harmonic amplitudes will depend upon the D.C. Stark field bias and the laser operating frequency. Additional consideration must be given to the absorber pressure, since dipole/dipole long range interactions produce appreciable collision broadening even at low pressures.

We have observed modulator harmonic distortion in several Stark effect gasses, both inside and outside the laser cavity. Of particular interest is the behavior of 1-1 Difluoroethane as a

function of varying A.C. and D.C. Stark field amplitudes. Figure 3.4 shows the variation of modulator response with A.C. field amplitude. These data clearly show a gradual increase in harmonic distortion with A.C. field strength. For this particular gas/cell combination, the first harmonic appears at about 50 volts peak to peak, and second harmonic content becomes strong at about 400 volts p-p. The distribution of harmonic energy can also be varied by changing the D.C. bias while holding the A.C. field constant, as shown in Figure 3.5. Close inspection of these results shows that the fundamental response which is observed at zero bias reappears at about 150 volts of D.C. field, but 180° out of phase with the zero bias response. It appears then that this bias change is just that necessary to shift the absorption profile across the fixed laser frequency. Further increases of D.C. bias show a repetition of this behavior, suggesting that two closely spaced absorption lines contribute to the modulation of P(20) by 1-1 difluoroethane.

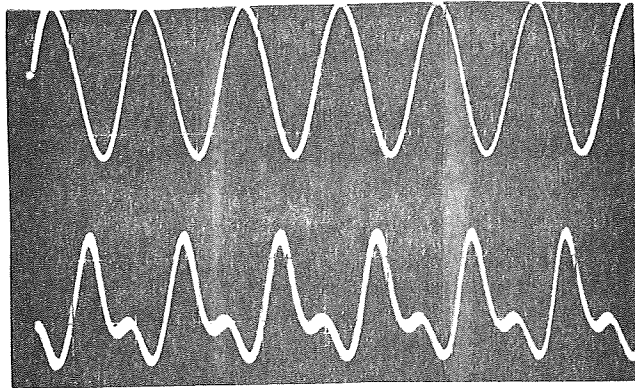
Although the data shown here represent intracavity modulation, similar results are obtained when the cell is outside the cavity. The observed modulation depths are about an order of magnitude smaller in the latter case, however, since the absorption must now reduce the emitted light rather than the single pass cavity feedback field.



Drive: 10 v/cm

DC Zero

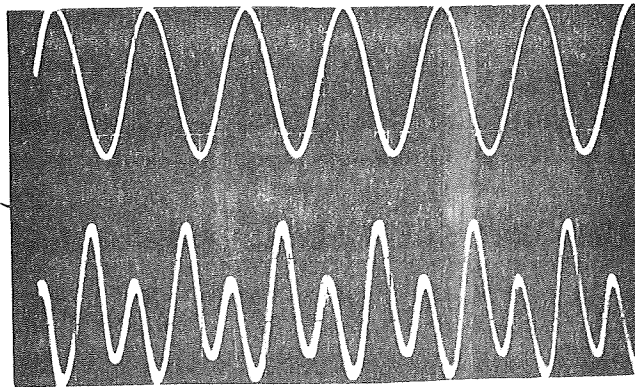
Response: 1 mv/cm



Drive: 20 v/cm

DC Zero

Response: 2 mv/cm

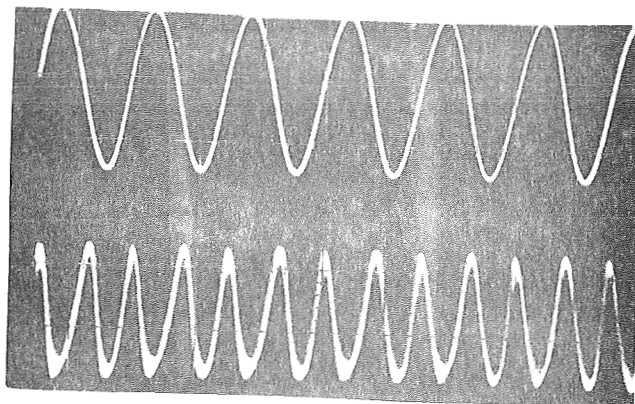


Drive: 50 v/cm

DC Zero

Response: 10 mv/cm

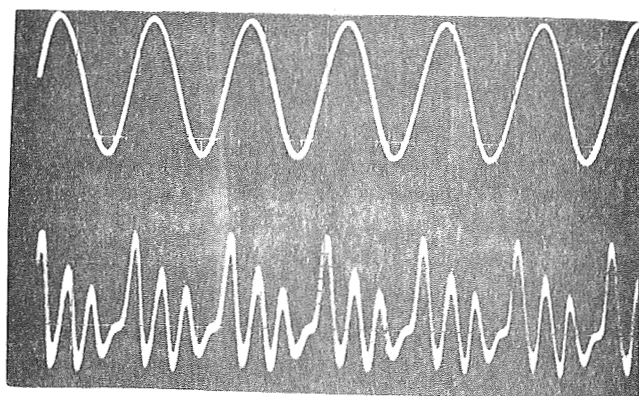
Figure 3.4. Stark Modulation Response vs. AC Field Variation.



Drive: 100 v/cm

Zero DC

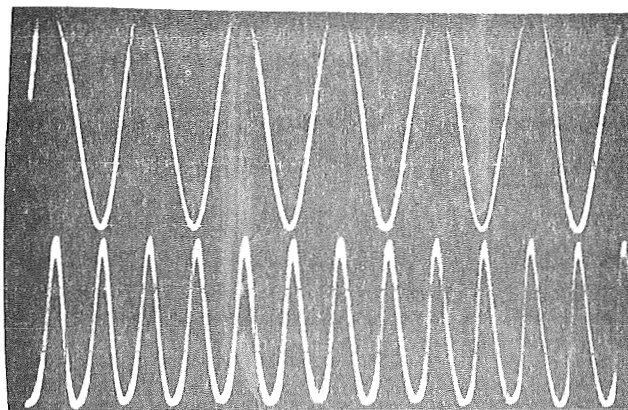
Response: 20 mv/cm



Drive: 200 v/cm

Zero DC

Response: 10 mv/cm



Drive: 200 v/cm

Response: 50 mv/cm

Figure 3.4

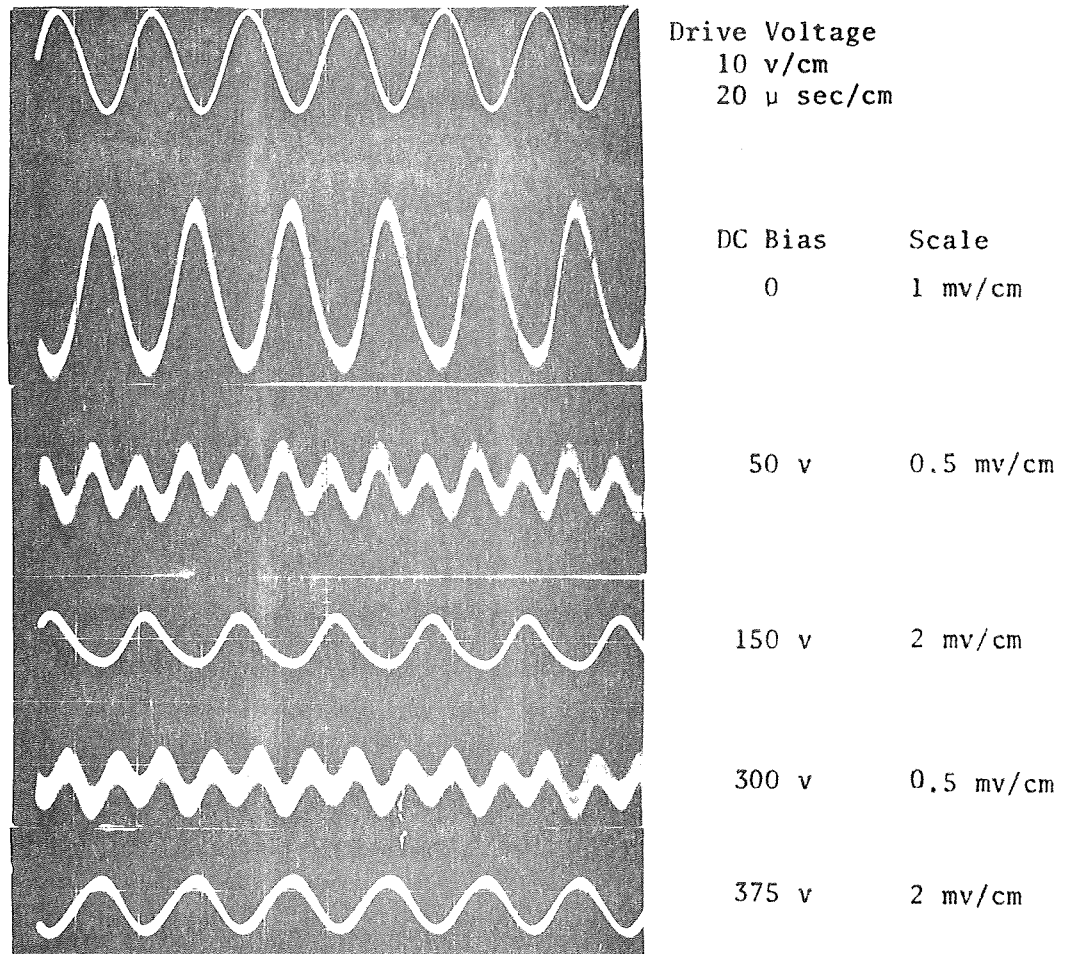


Figure 3.5 Stark Modulation Response vs. DC Bias Variation.

At the highest drive voltages used during intracavity modulation, the modulation depth of the laser output approaches 100%. On the basis of this result, it appears that the use of suitable pressures and A.C. modulation waveforms will produce driven Q switching of a CO₂ laser. For systems intending to use pulse modulation transmission, this mode would be particularly attractive because of the increased laser output obtainable.

4. COMPETITION BETWEEN TRANSITIONS IN A CO₂ LASER

4.1 The CO₂ Laser Signature Problem

A CO₂ laser may oscillate at any one of many possible lines. As the cavity length of such a laser is varied over a distance $\lambda/2$, a large number of such lines oscillate one at a time in succession. The listing of the identities of such sequences of lines constitutes a "signature" of the laser and is a matter of practical importance in the operation of such lasers in remote controlled applications without the use of line selecting elements in the laser cavity.

4.2 Apparatus and Experiments

A reasonably stable CO₂ laser was constructed specifically for these experiments. The laser cavity consisted of two stainless steel discs separated by three 23" Invar rods of $3/4$ " diameter. The cavity mirrors were mounted on the discs with a mirror separation of approximately 23". The output mirror was a germanium flat dielectrically coated for 80% reflection at 10.6 μ . The second surface of the flat was A/R coated to prevent spurious Fresnel reflection at the germanium - air boundary. The other cavity mirror was a 4 m Pyrex substrate with Au coating, mounted on a 20 element piezoelectric translator. The gain cell was a 15 inch x 5 mm Pyrex tube with NaCl Brewster windows, water jacket and Ni

cathode. The tube was clamped in two places to one of the Invar spacers. Vacuum and water lines were connected with Tygon tubing to minimize mechanical coupling into the cavity. Air spaces at both ends of the resonator were enclosed by Mylar drift tubes to minimize the effect of convection currents. Laser output power was in the range of about 750 mw to 1.2 watts.

The experimental apparatus was arranged as shown in Figure 4.1. This arrangement allowed the simultaneous display of the entire laser output vs. cavity length "signature" as well as identification of any component element in terms of a particular laser line. The cavity length was tuned over $\lambda/2$ for the following sequences of parameter changes.

- A. "Signature" or line sequence versus pressure with discharge current adjusted to provide maximum laser output at each pressure.
- B. "Signature" versus discharge current at constant pressure.
- C. Effect of gross changes in cavity length.
- D. Effect of insertion of loss in the laser cavity in the form of a NaCl disc, and also in the form of an unevenly heated NaCl disc.
- E. Effect of gross changes in pressure.

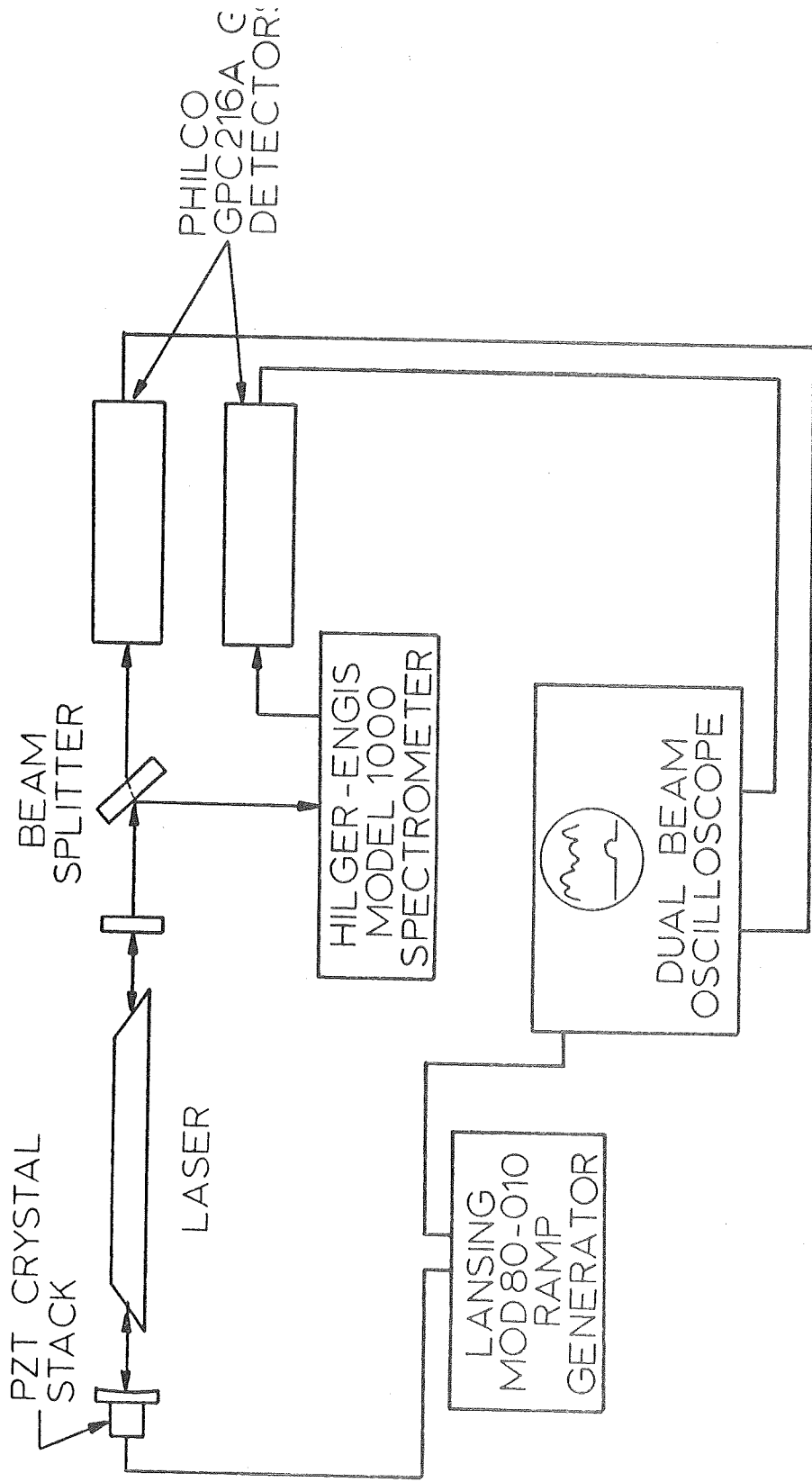


Figure 4.1 Apparatus for Laser Signature Experiments.

Although the variation of these parameters produces complex changes in individual "signatures", it is nevertheless remarkable that except in two extreme cases, the lines P(16) and P(20) of the 10.6μ CO_2 band always appear if the cavity is swept about $\lambda/2$.

4.3 Experimental Results

The sequence of Figures 4.2 through 4.10 show the changes in line sequence as the laser pressure was reduced in 1 Torr increments from 18 Torr to 10 Torr. In each case the current was readjusted to optimize laser action. In all cases the gas fill was 4.65 percent H_2 , 17.5 percent N_2 , 16.9 percent CO_2 and 60.95 percent He by partial pressure.

Figures 4.11 through 4.17 illustrate the effect of variation in discharge current at constant pressure. The last of this sequence, taken at very low excitation levels, shows especially well the very high gain of P(16) and P(20).

The effects of large and arbitrary changes in cavity length are shown in Figures 4.18 - 4.21. Note that although the line sequence is drastically altered by these changes, P(16) and P(20) still survive very well.

Figures 4.22 and 4.23 demonstrate the changes in signature brought about by a fresh fill of laser gas. Although the

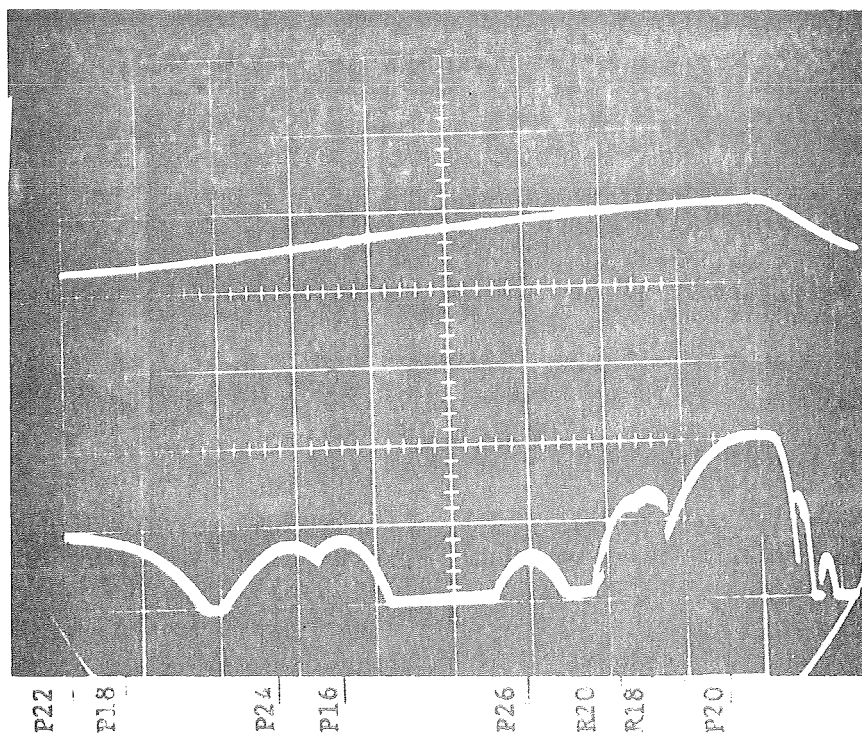


Figure 4.2

P = 18 Torr

I = 11 ma.

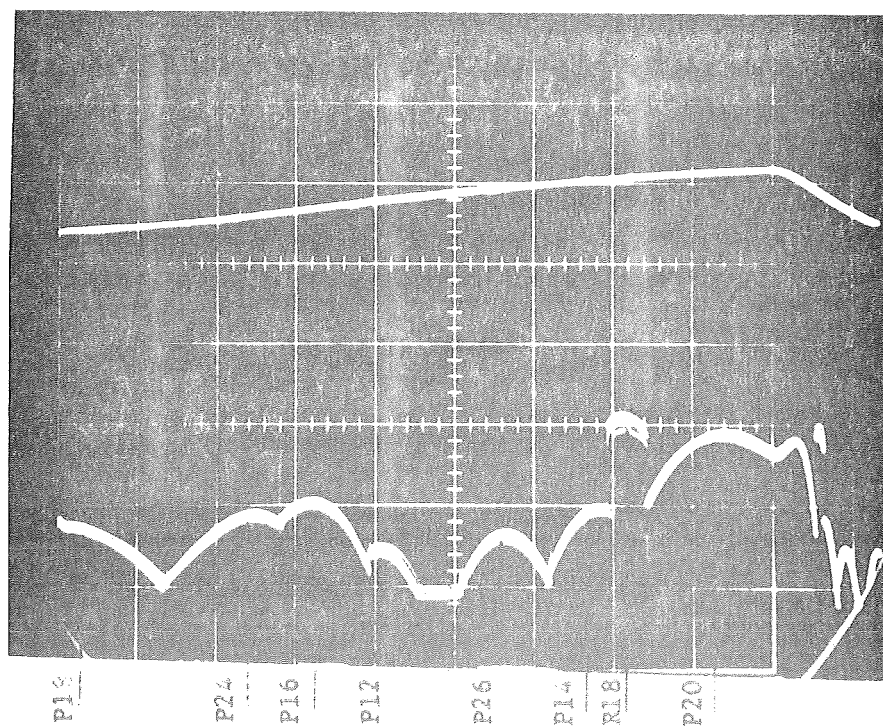


Figure 4.3

P = 17 Torr

I = 10 ma.

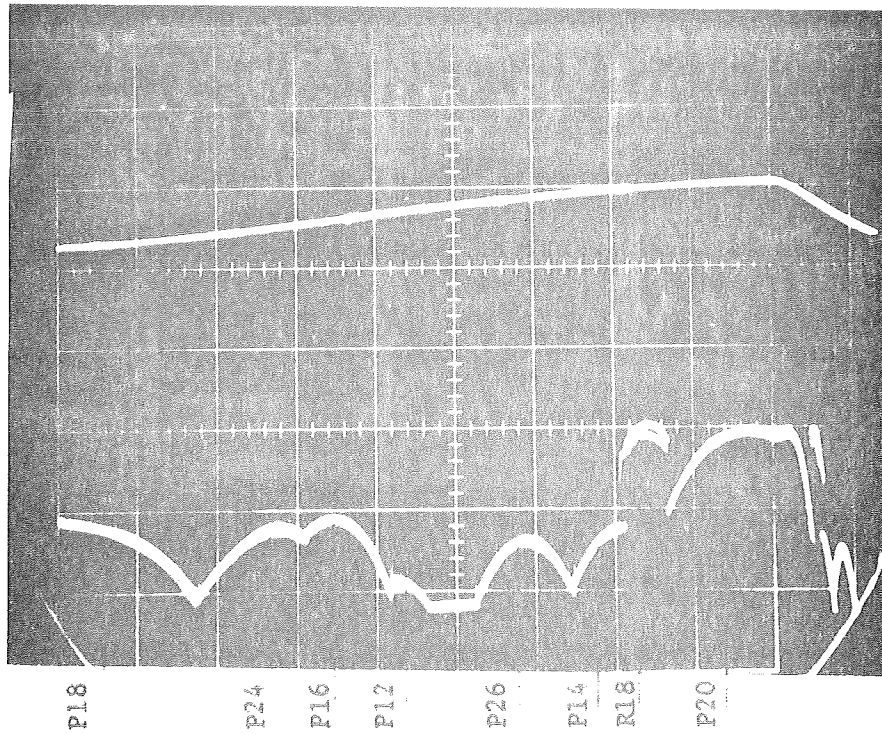


Figure 4.4

P = 16 Torr

I = 10 ma.

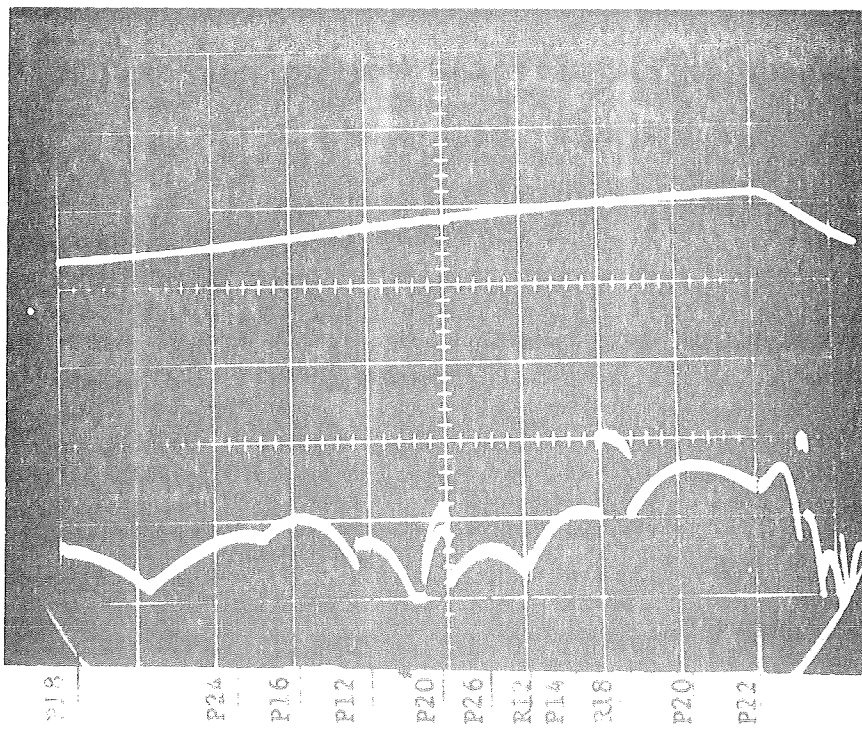


Figure 4.5

P = 15 Torr

I = 8 ma.

* Indicates lines of 9.4 μ band

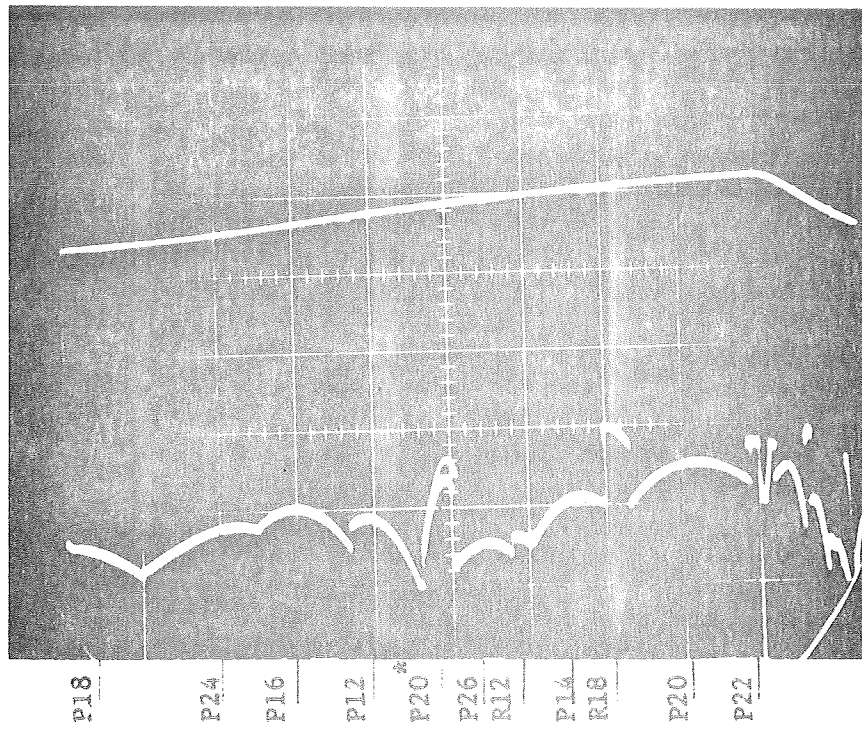


Figure 4.6

P = 14 Torr

I = 7.8 ma.

* Indicates lines of 9.4μ band

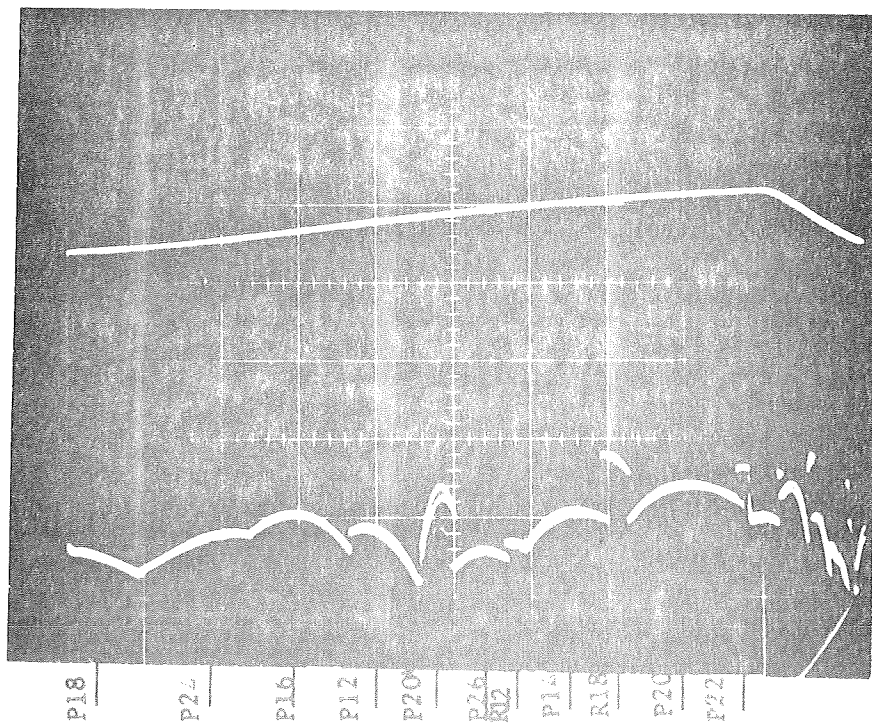


Figure 4.7

P = 13 Torr

I = 6.8 ma.

* Indicates lines of 9.4μ band

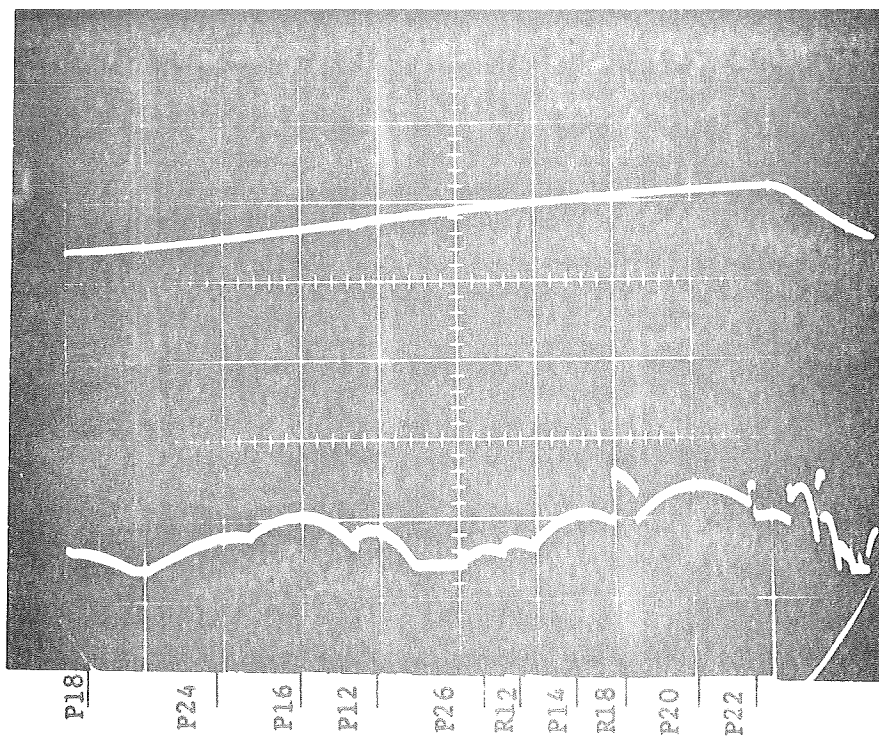


Figure 4.8

P = 12 Torr

I = 6 ma.

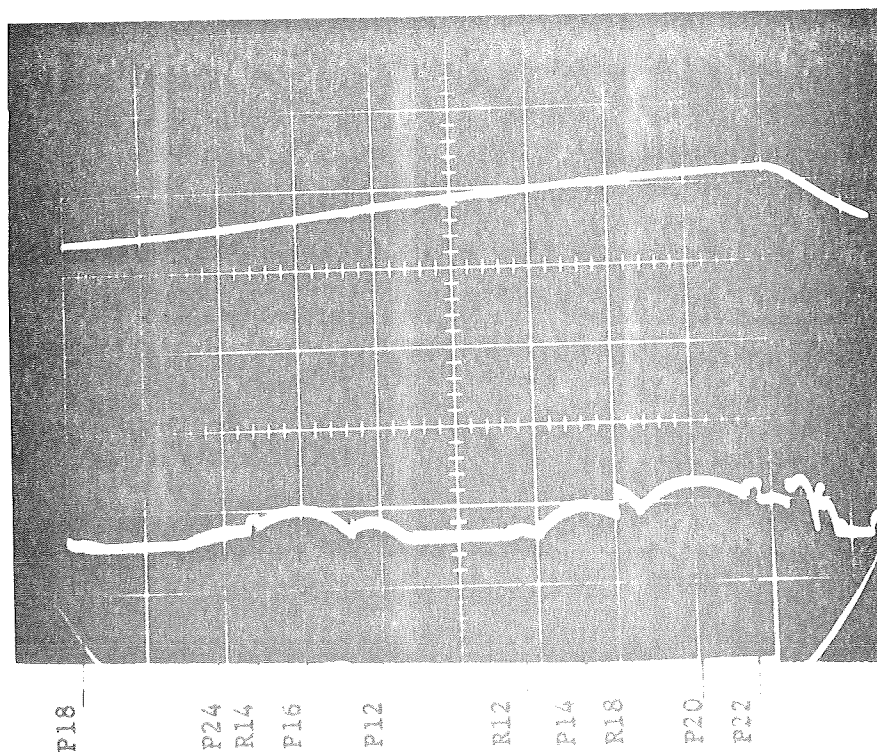


Figure 4.9

P = 11 Torr

I = 5 ma.

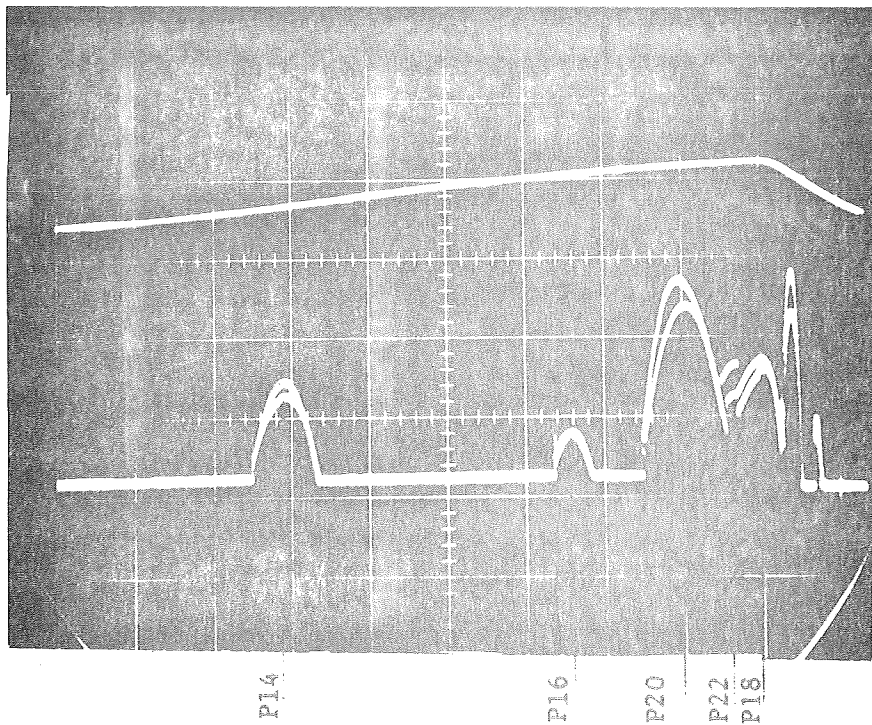


Figure 4.10
P = 10 Torr
I = 4.4 ma.

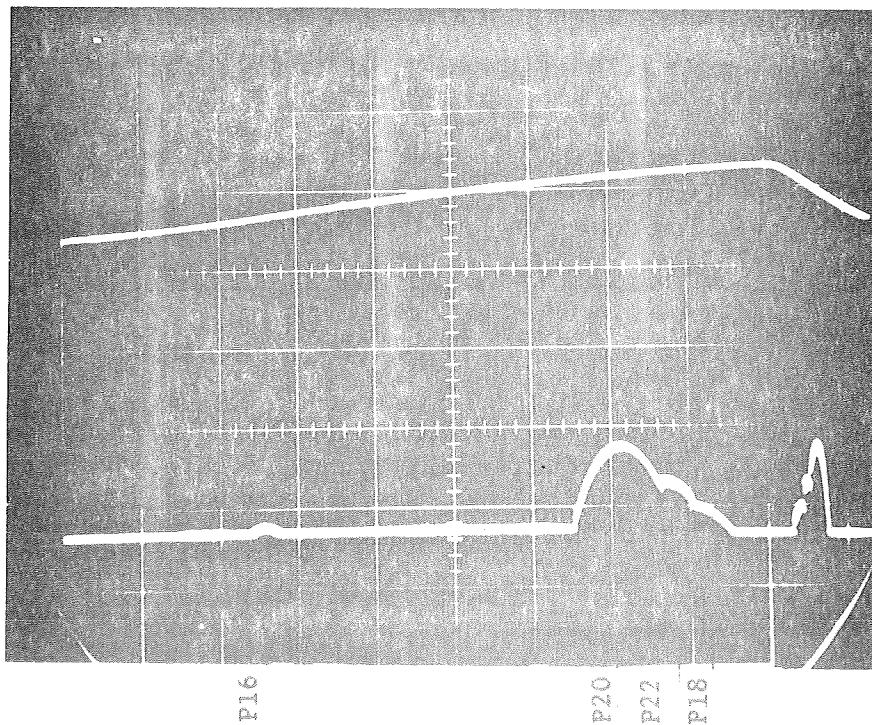


Figure 4.11
P = 15 Torr
I = 11 ma.

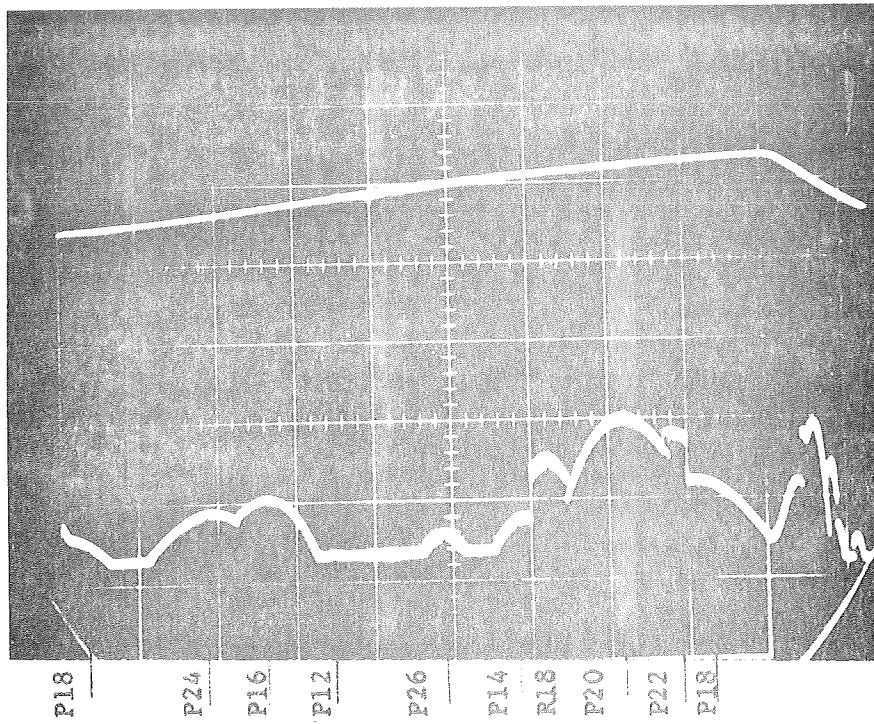


Figure 4.12

P = 15 Torr

I = 10 ma.

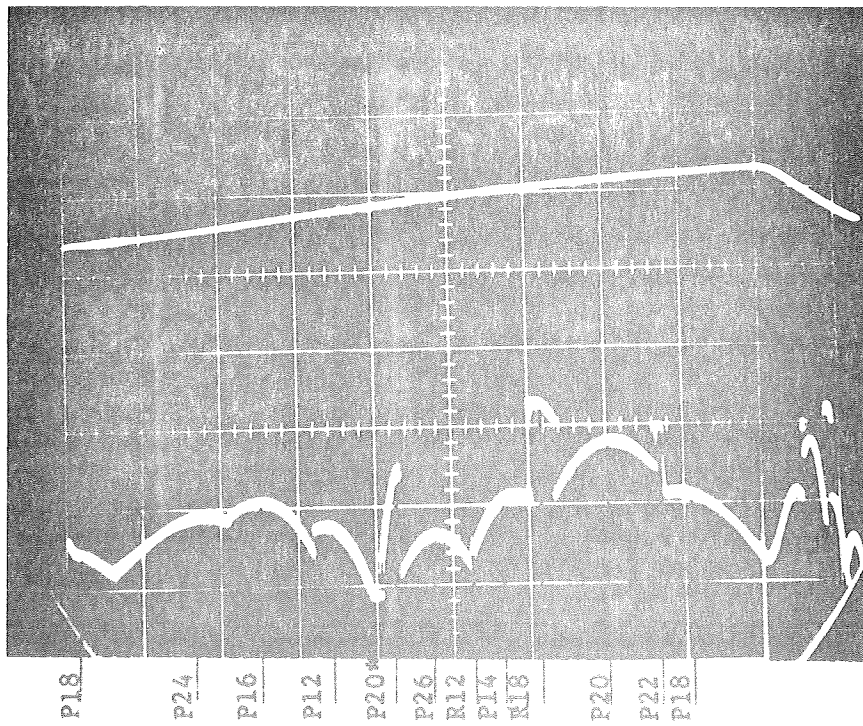


Figure 4.13

P = 15 Torr

I = 9 ma.

* Indicates lines of 9.4 μ band

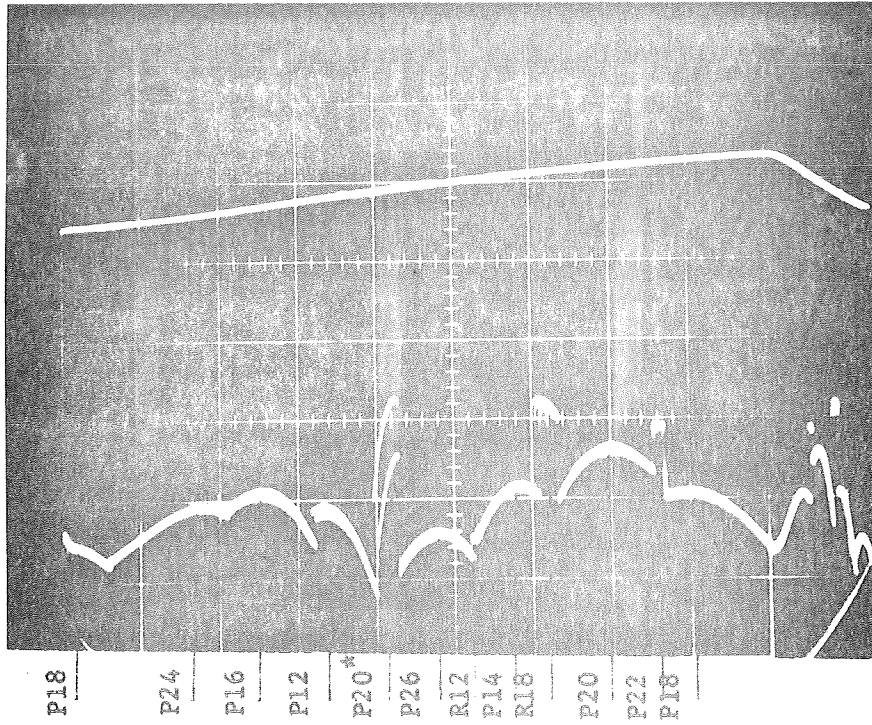


Figure 4.14

P = 15 Torr

I = 8 ma.

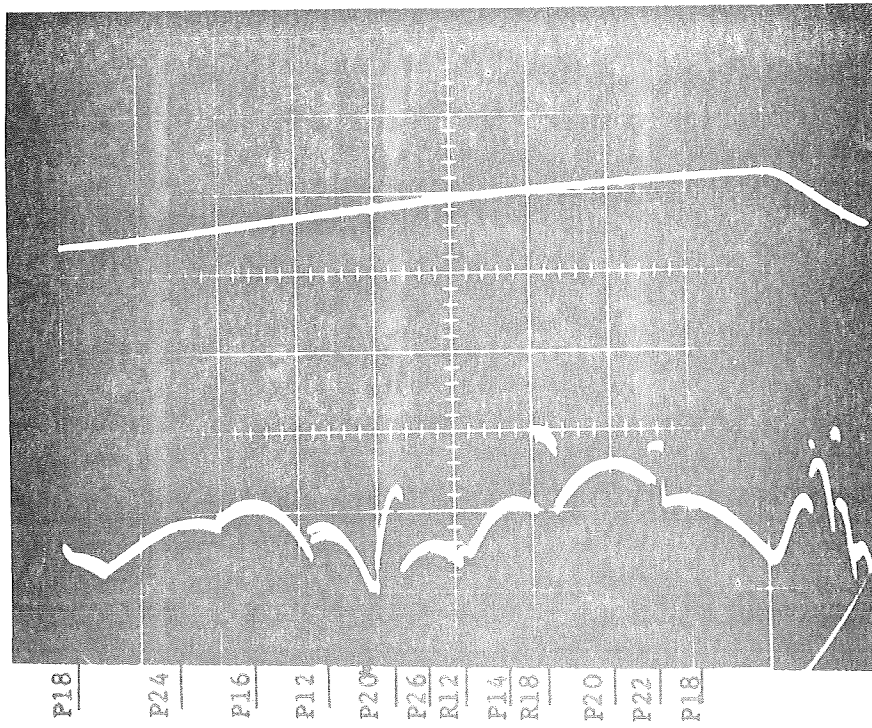


Figure 4.15

P = 15 Torr

I = 7 ma.

* Indicates lines of 9.4 μ band

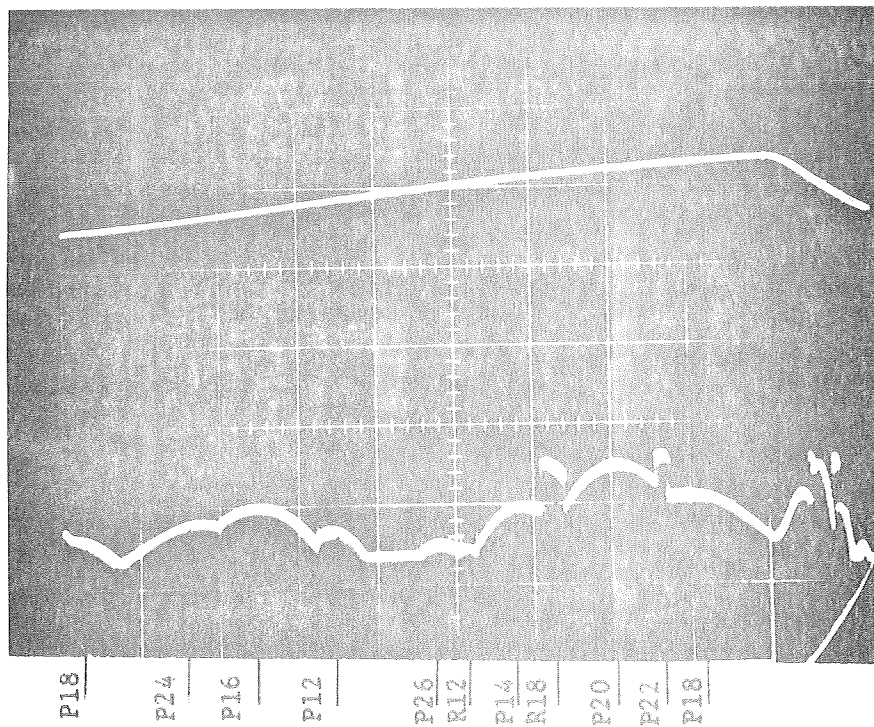


Figure 4.16

P = 15 Torr

I = 6 ma.

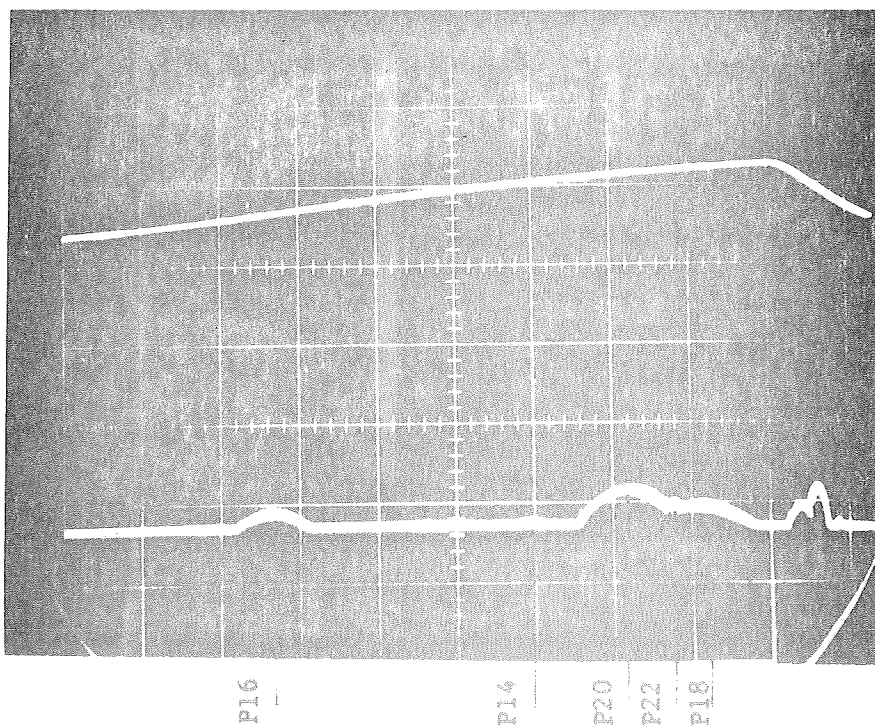


Figure 4.17

P = 15 Torr

I = 5 ma.

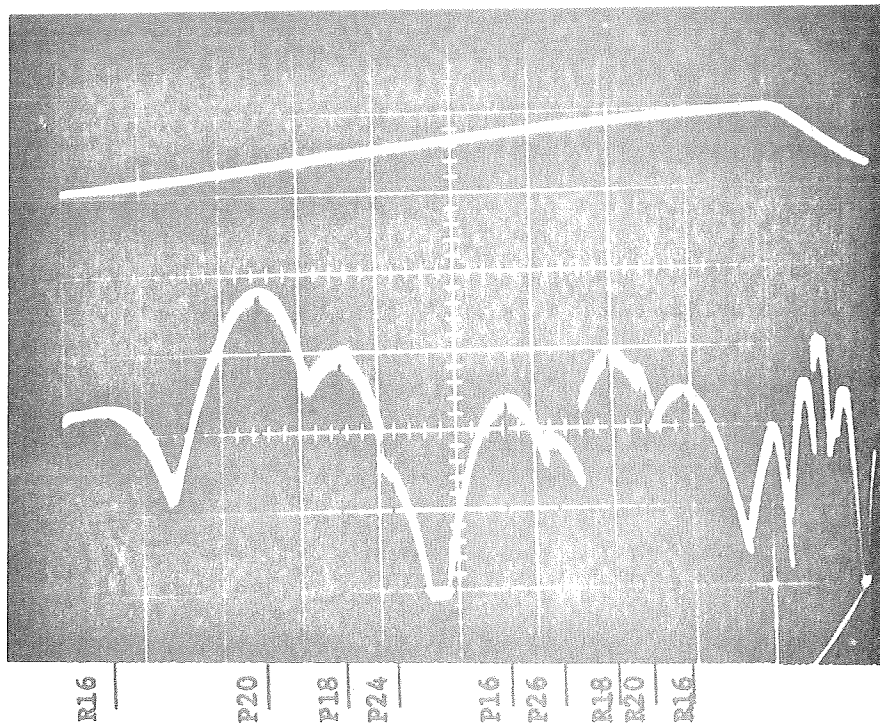


Figure 4.18

P = 15 Torr

I = 10 ma.

Cavity length = L

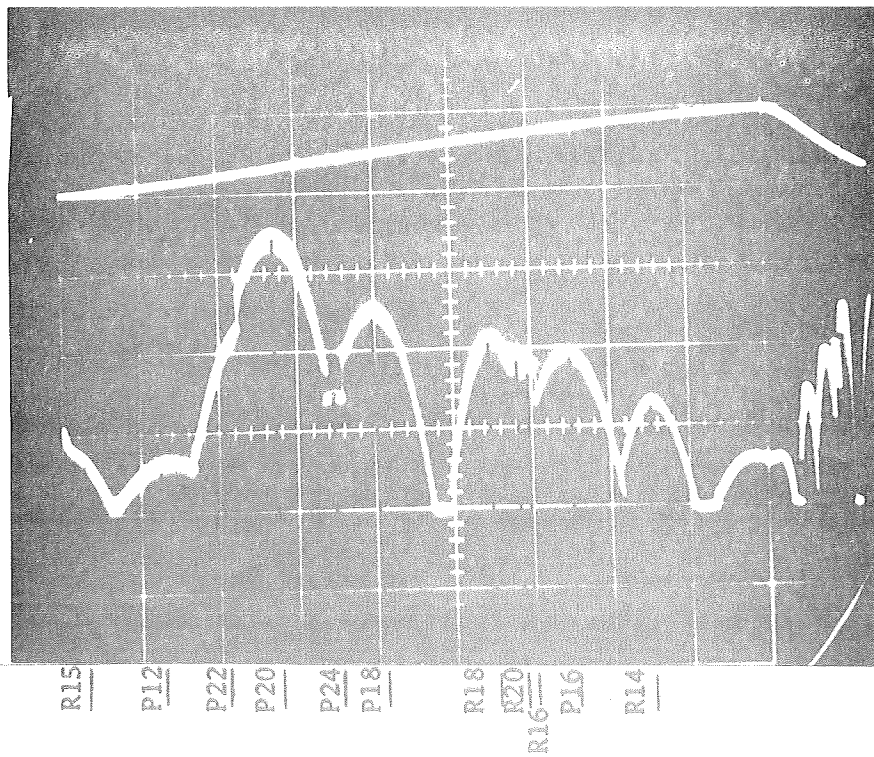


Figure 4.19

P = 15 Torr

Cavity length = L + 100 μ

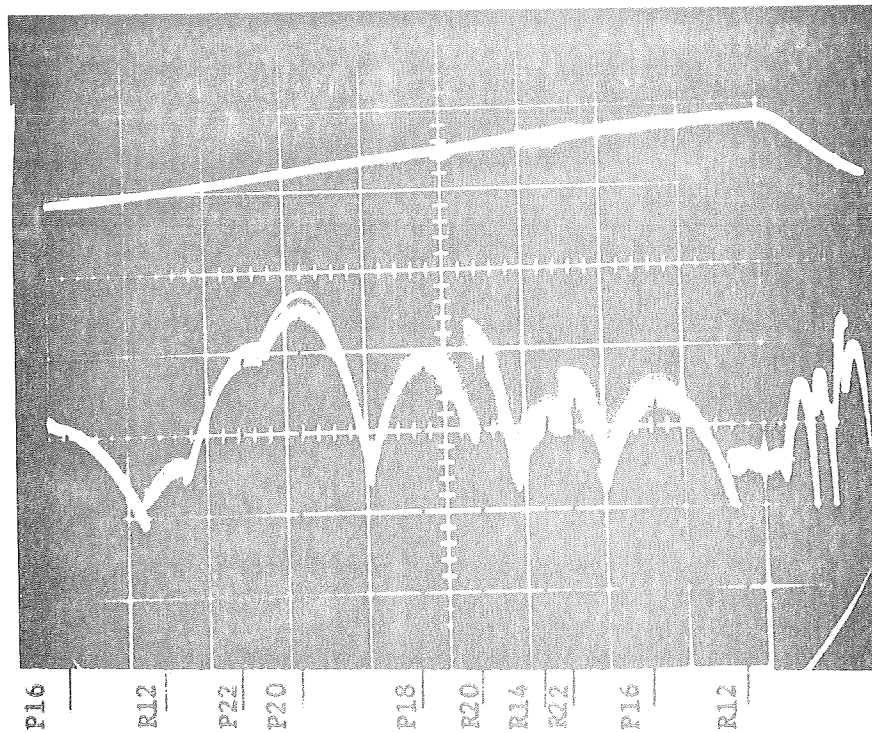


Figure 4.20

P = 15 Torr

I = 10 ma.

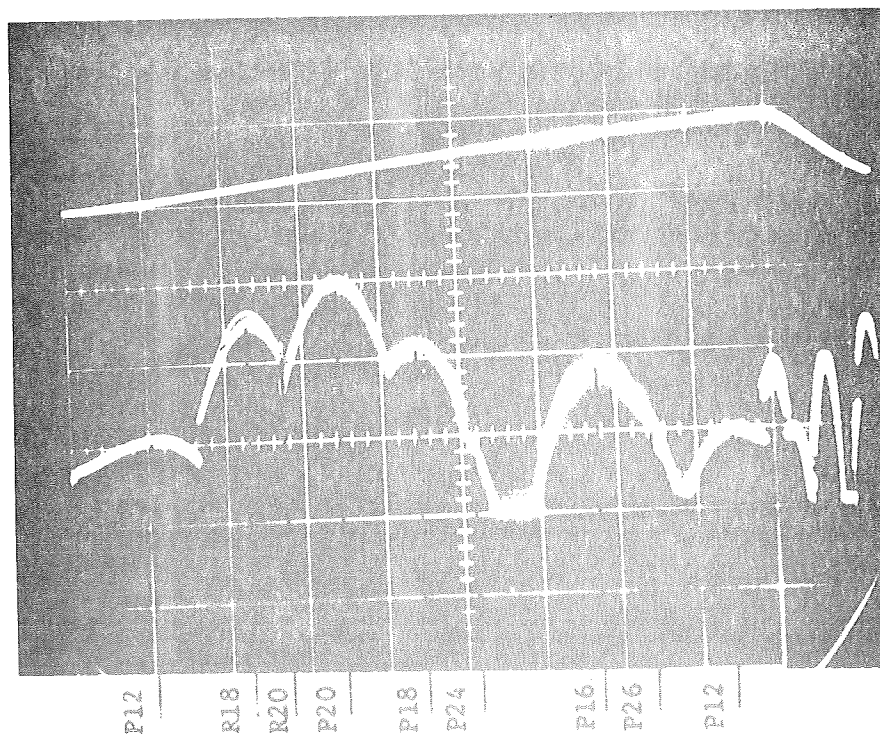
Cavity length = $L + 200\mu$ 

Figure 4.21

P = 15 Torr

I = 10 ma.

Cavity length = L

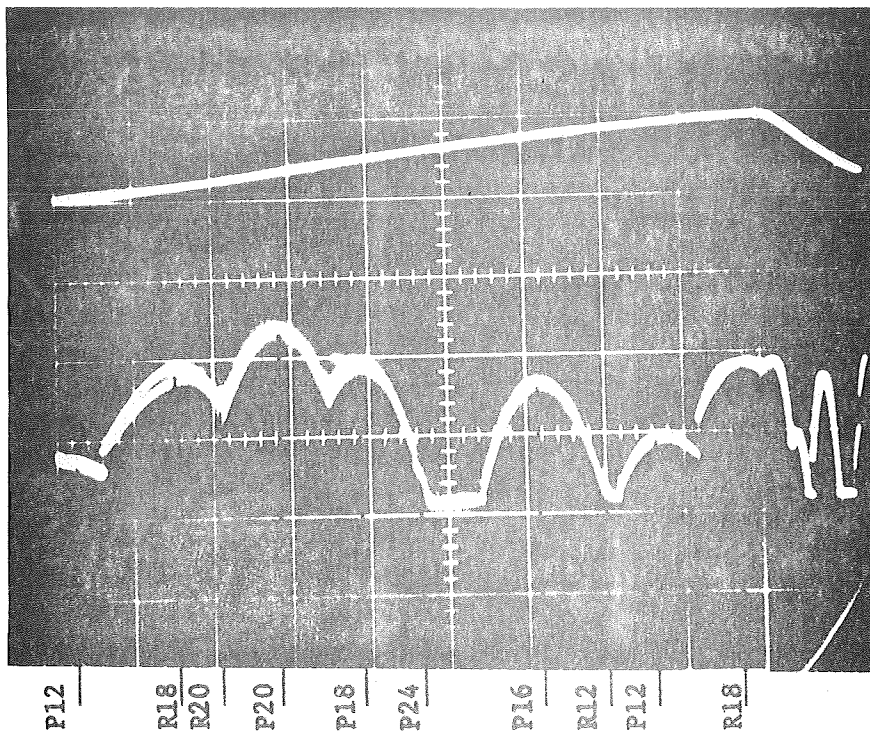


Figure 4.22

P = 15 Torr

I = 7 ma.

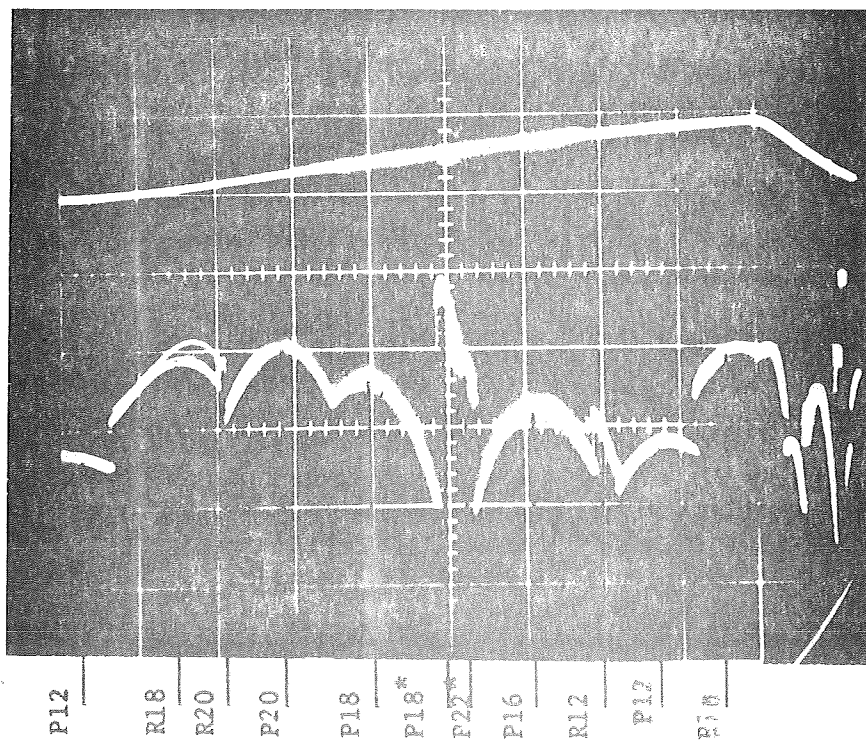


Figure 4.23

P = 15 Torr (fresh gas)

I = 6 ma.

* Indicates lines of 9.4 μ band

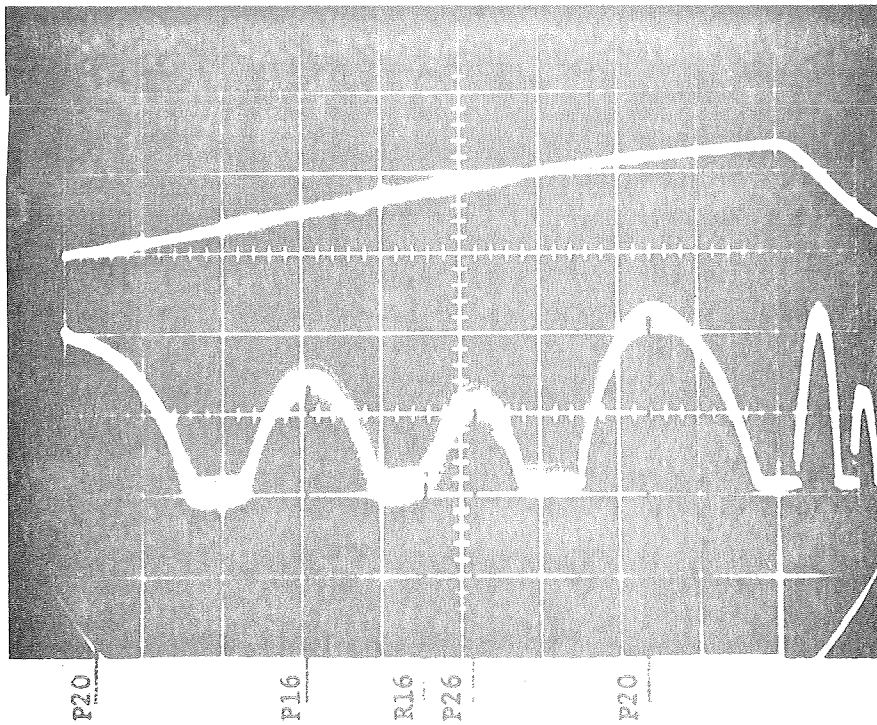


Figure 4.24

P = 15 Torr

I = 6 ma.

Polished NaCl flat in cavity

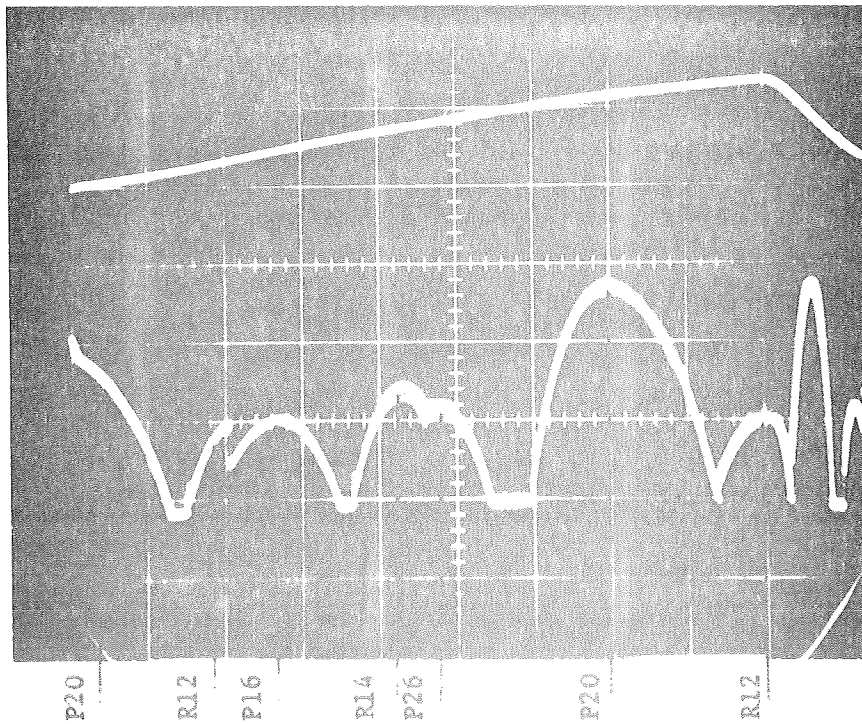


Figure 4.25

P = 15 Torr

I = 6 ma.

Polished NaCl flat in cavity,
small temperature gradient in flat.

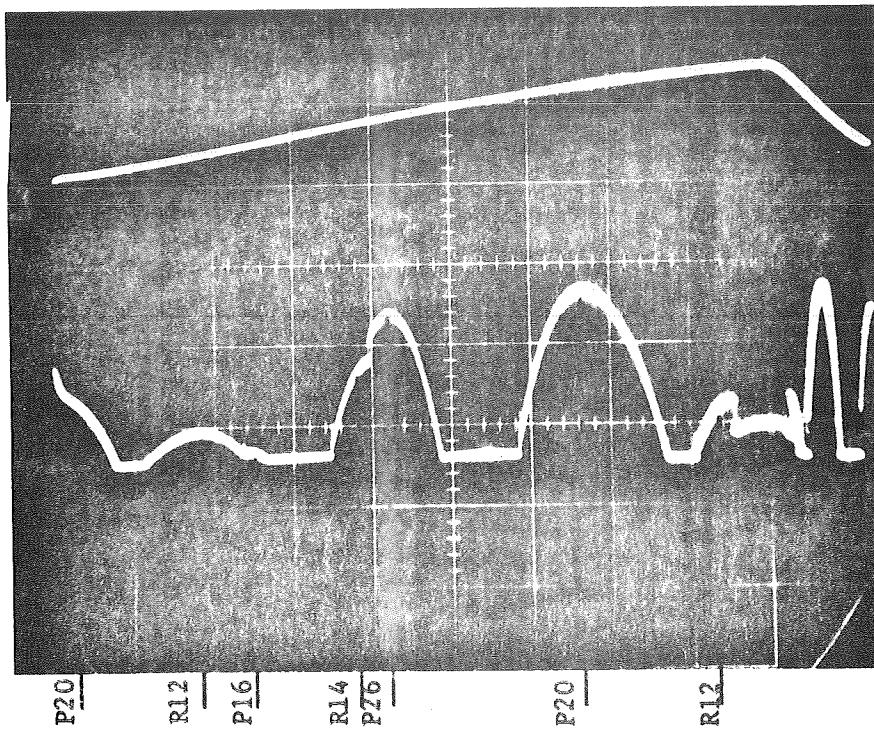


Figure 4.26

P = 15 Torr

I = 6 ma.

Polished NaCl flat in cavity,
 large temperature gradient in flat.

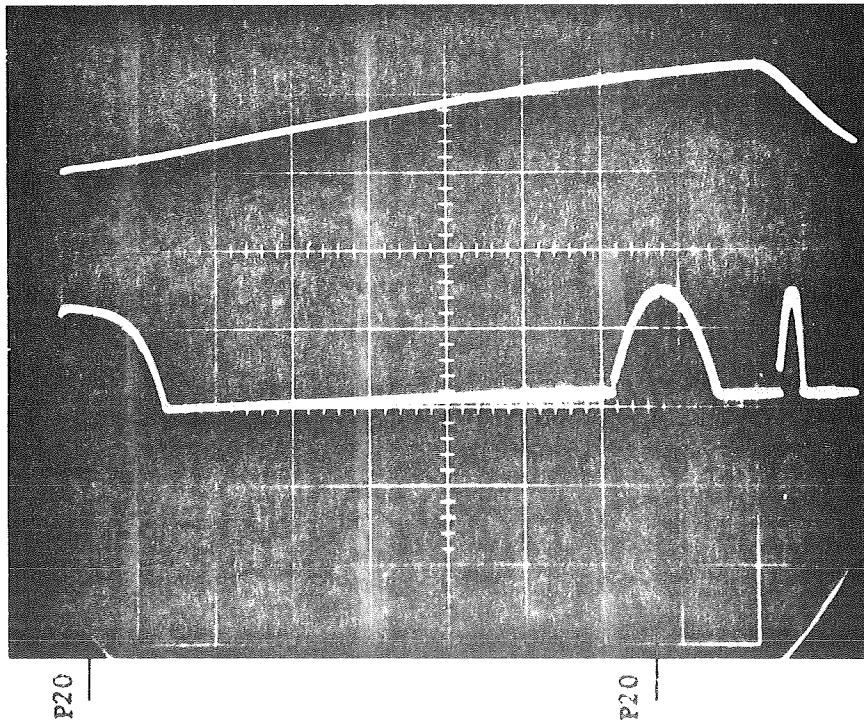


Figure 4.27

P = 30 Torr

I = 10 ma.

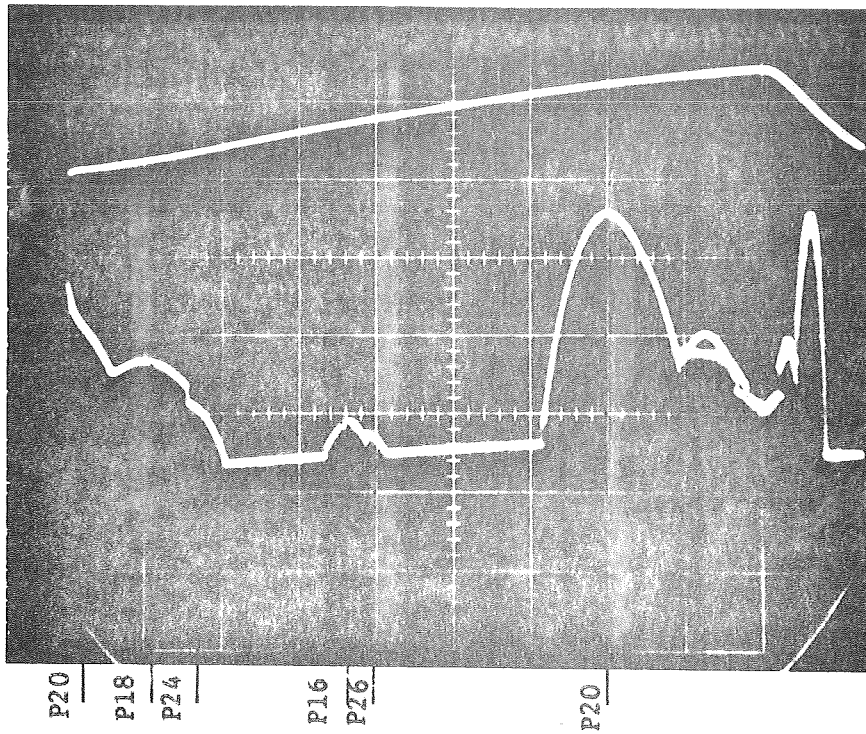


Figure 4.28

P = 25 Torr

I = 10 ma.

optimum current is reduced ($\sim 6\text{ma}$ vs. $\sim 10\text{ma}$), there is no change in the presence of P(16) and P(20).

A 5 mm thick NaCl window was inserted into the laser cavity to examine the effects of additional cavity losses. Figures 4.24 through 4.26 illustrate these results. The second and third signatures are those observed when the NaCl disc was heated at one point to produce moderate and then severe temperature gradients in the disc.

In the final two oscillograms, Figures 4.27 and 4.28, the effects of very high pressure are shown. It is seen that P(20), is always present if laser action occurs at all, but that P(16) does not appear above about 26 Torr.

4.4 Discussion of Results

The results of this investigation show that in applications which require remote switching on and off of CO_2 lasers, operation on either P(16) or P(20) of the 10.6μ band is most advisable, since these lines always appear within the laser "signature". Such lasers will operate effectively provided that additional equipment is available which can recognize the presence of laser oscillation on, say, P(20) and if a feedback system is arranged to automatically tune the cavity length as required to maintain this condition. Lock in reference may be to the lasing line center or to an external absorption cell containing another molecular gas.

5. VERY HIGH RESOLUTION INVERTED LAMB DIP SPECTRA OF SF₆

5.1 Background of Investigation

The technique of inverted Lamb dip spectroscopy, as first described by Lee and Skolnik⁴, offers a powerful advantage in absorption spectroscopy of gases. This method improves the ultimate resolution from the Doppler linewidth to the homogeneous width of the particular species involved. For a great many gases, this results in a resolution improvement of one to several orders of magnitude. Applying this technique to the 10 μ spectroscopy of SF₆, Rabinowitz, Keller, and LaFourrette⁵ have reported from 1 to 4 absorption lines coincident with selected P branch lines of the 10.6 μ CO₂ laser. According to Burak, Steinfeld, and Sutton⁶, however, one should expect denser SF₆ line spectra in this region.

Refinement of the technique of inverted Lamb dip spectroscopy combined with heterodyne methods has enabled us to observe and measure SF₆ line spectra with spacings of about 1 MHz. The observed high line density results from the large molecular mass of SF₆, the Coriolis splitting of the triply degenerate upper vibrational level, the removal of the "K" degeneracy by Coriolis interactions⁷, and the presence of hotband transitions.⁸

5.2 Apparatus and Experiments

The experimental apparatus is indicated in Figure 5.1. Two sealed off CO₂ lasers (CO₂/N₂/He/H₂ = 2.8/2.8/9.7/0.7 Torr) were operated in identical resonators consisting of a grating for line selection, a specially designed 60 cm quartz spacer, and a piezoelectrically driven mirror for cavity length tuning. The lasers, which operate single mode, had a short term relative passive stability of 1:10⁹. The output from one laser entered an overlapping double pass absorption cell with a total path length of 80 cm and an SF₆ pressure of 50 m Torr. The beam diameter is restricted by mirror geometry to less than 5 mm. Maximization of beam overlap volume in the absorption cell optimized the amplitudes of inverted Lamb dips at SF₆ absorption resonances. A Philco GPC-216A Ge: Au detector was used both for direct detection, and also for heterodyne detection through use of the second laser as a local oscillator.

The absorption line frequency spacings were determined in the following manner. While the local oscillator laser was biased at a convenient reference frequency, the probe laser was repetitively scanned 10 MHz over a one second period by application of the oscilloscope sawtooth voltage to the cavity mirror tuner. The resulting inverted Lamb dip pattern was displayed after selective amplification. A typical pattern is shown in Figure 5.2.

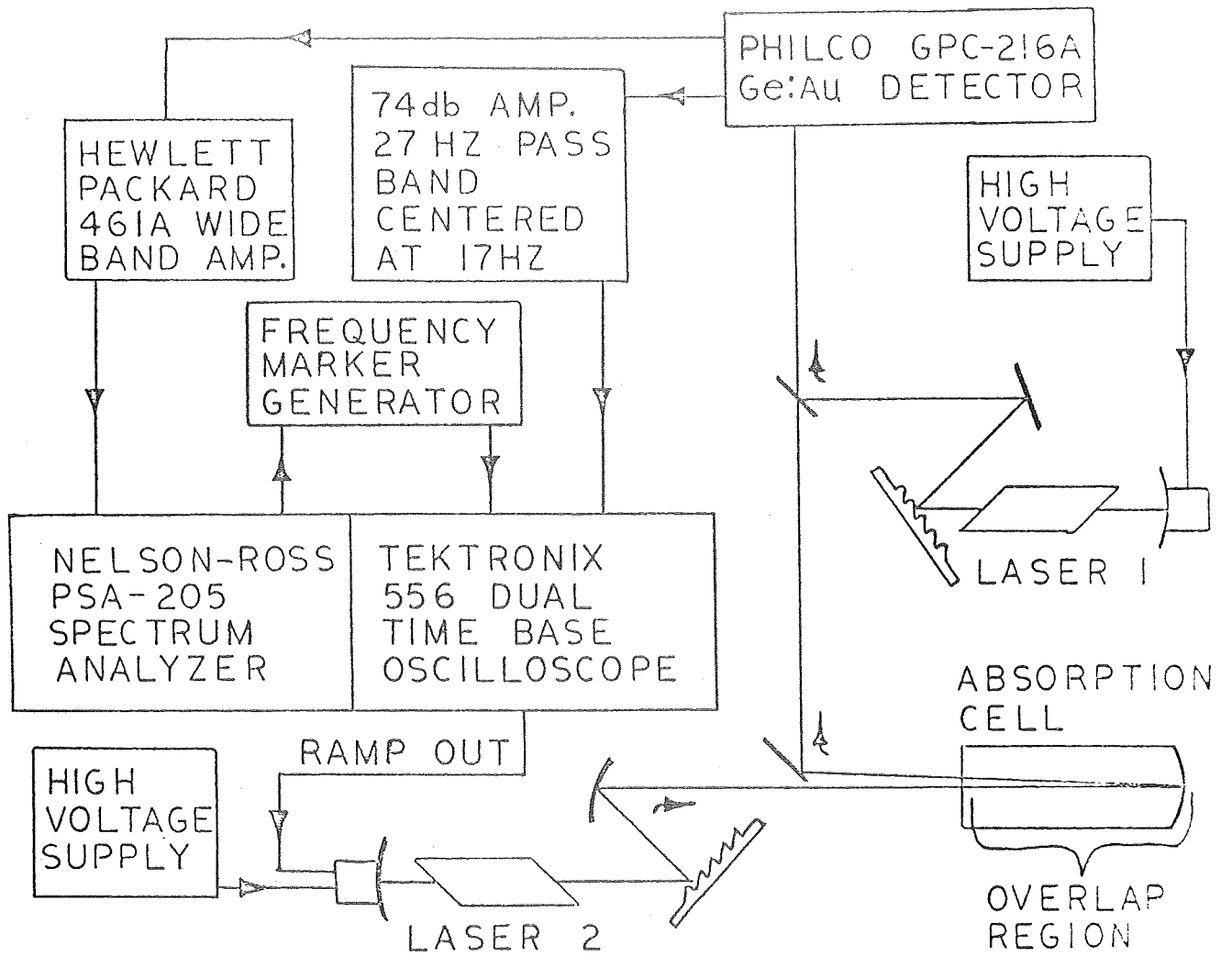


Figure 5.1 Apparatus for Inverted Lamb Dip Absorption Spectroscopy.

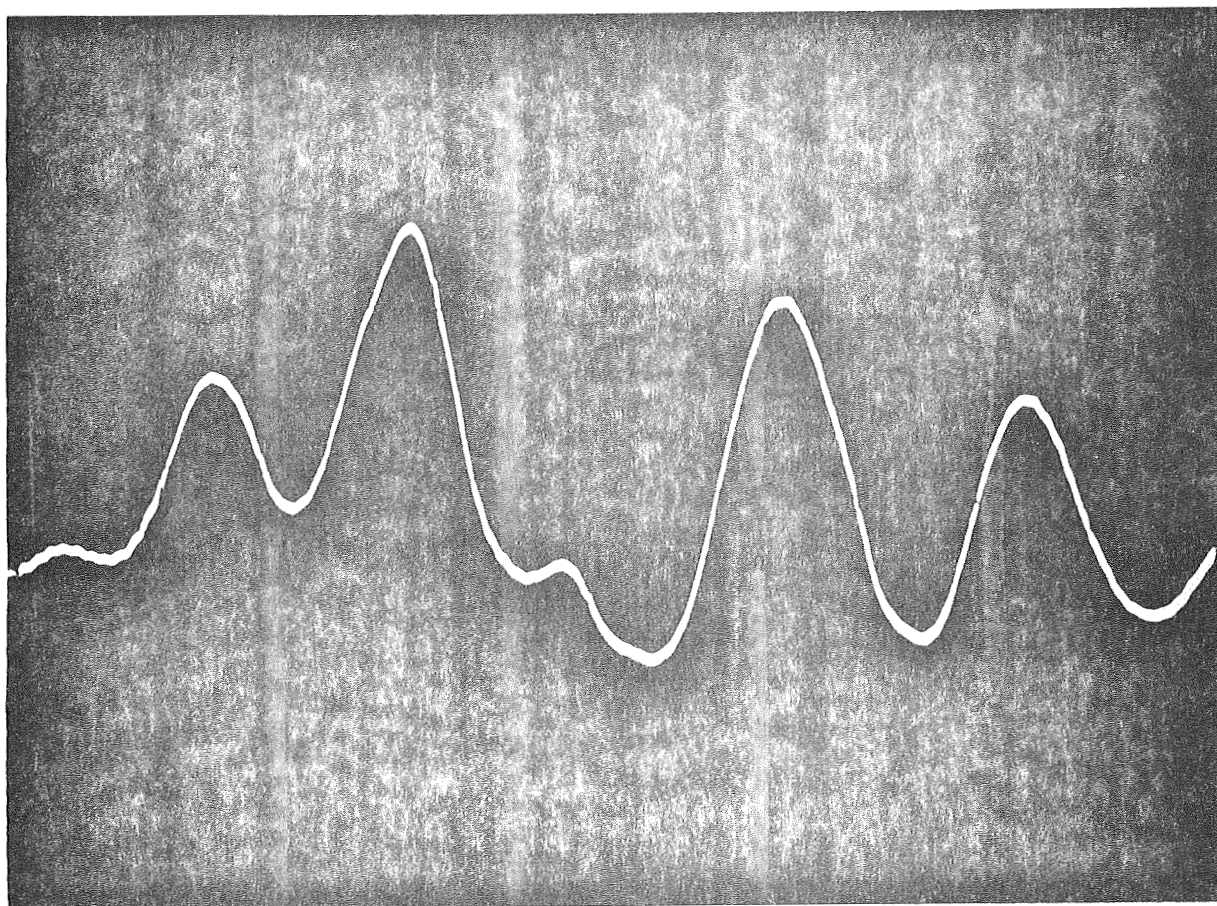


Figure 5.2 Typical Absorption Spectrum.

The beat frequency between the lasers was continuously monitored by a Nelson-Ross Model PSA 205 Spectrum Analyzer operating at 15 scans/second. Whenever the analyzer tuned through the lasers beat frequency, a marker pulse was introduced on the oscilloscope output. The resulting series of marker pulses, once calibrated from the spectrum analyzer trace, formed a frequency scale from which the separations between neighboring inverted Lamb dips could be determined.

Sequential biasing of the 10 MHz scanning window across the entire laser gain curve produced data which were assembled to form the composite spectra shown in Figures 5.3 and 5.4. Sufficient runs were made to facilitate the calculation of a meaningful average for each reported frequency separation. Based on the average deviations of these runs, we estimate the reported values to be accurate to ± 0.1 MHz. These separations appear in Tables 5.1 and 5.2 as the differences between adjacent absorption line frequencies. The resulting line spectra are incomplete due to the tendency of the stronger lines to obscure nearby weak lines. This effect is particularly noticeable in Figure 5.4.

The resulting line spectra were referenced to the coincident CO_2 emission line centers using the following method. Using the usual technique of stabilization by electronic lock in on a zero slope point of the laser intensity profile, both lasers were

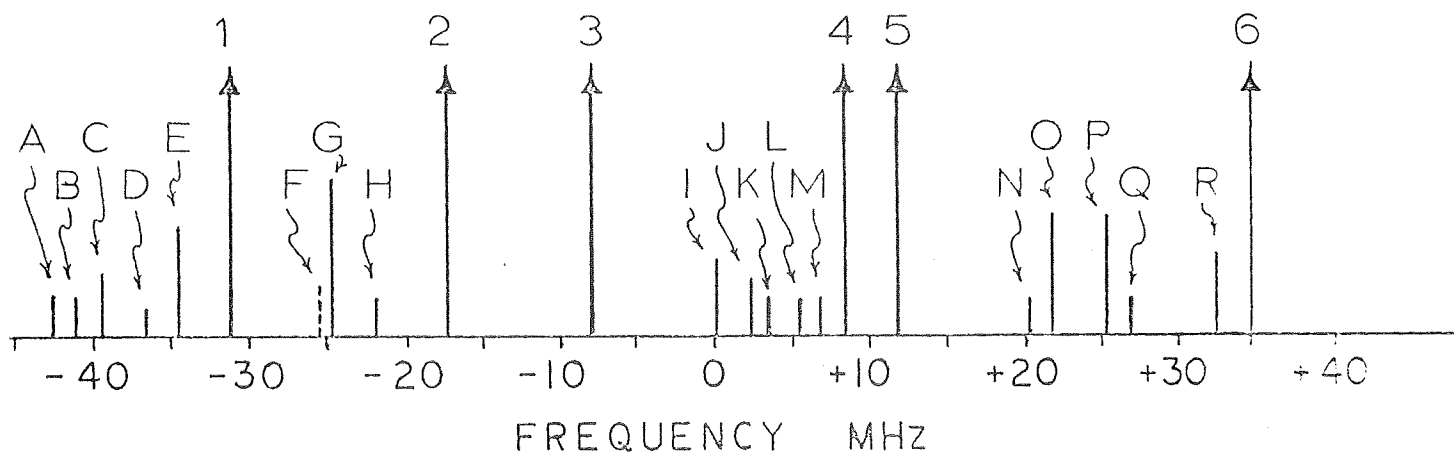


Figure 5.3 SF₆ Absorption Resonances Referred to the P(16) Line Center of CO₂.

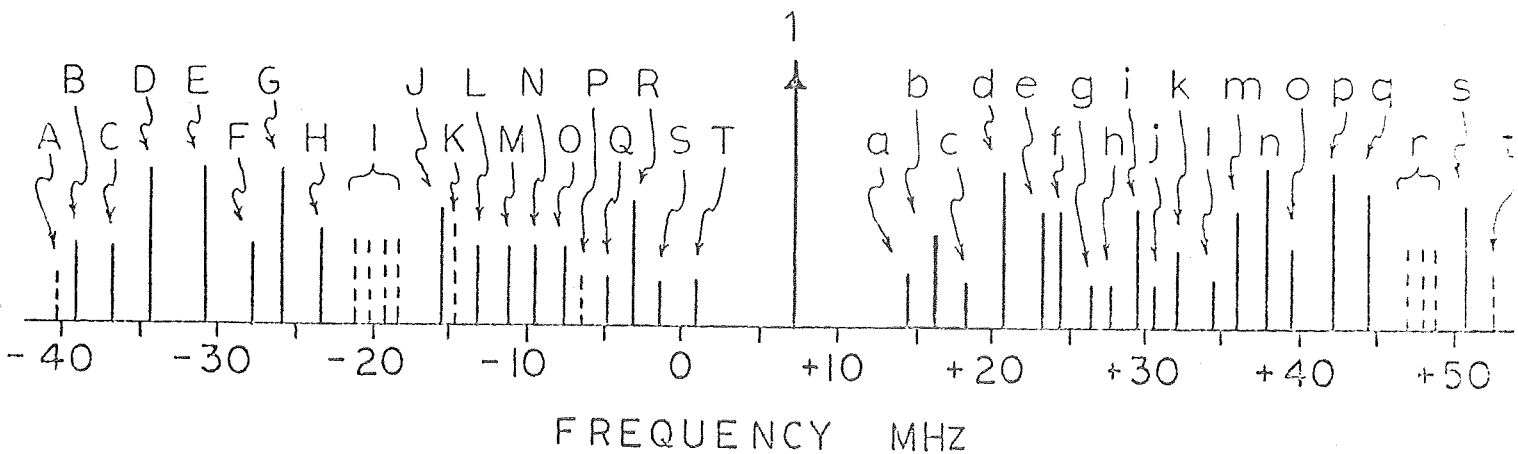


Figure 5.4 SF₆ Absorption Resonances Referred to the P(18) Line Center of CO₂.

Table 5.1 Observed SF₆ Absorption Line Centers Relative to the P(16) Line Center of CO₂. Line Designations are taken from Figure 5.3.

SF ₆ Line	Freq. MHz	SF ₆ Line	Freq. MHz	SF ₆ Line	Freq. MHz	SF ₆ Line	Freq. MHz
A	-42.33	F	-25.41	J	+ 2.53	N	+20.57
B	-41.43	G	-24.42	K	+ 3.84	O	+21.96
C	-39.38	H	-21.71	L	+ 5.52	P	+25.38
D	-36.93	2	-17.32	M	+ 6.71	Q	+26.96
E	-34.72	3	- 7.80	4	+ 8.81	R	+32.55
I	-31.07	I	+ 0.46	5	+11.96	6	+35.02

Table 5.2 Observed SF₆ Absorption Line Centers Relative to the P(18) Line Center of CO₂. Line Designations are taken from Figure 5.4.

SF ₆ Line	Freq. MHz	SF ₆ Line	Freq. MHz	SF ₆ Line	Freq. MHz	SF ₆ Line	Freq. MHz
A	-40.31	J	-15.40	l	+ 7.18	k	+32.05
B	-39.33	K	-14.73	a	+14.82	l	+34.12
C	-36.74	L	-13.18	b	+16.19	m	+35.85
D	-34.24	M	-11.38	c	+18.34	n	+37.90
E	-30.64	N	- 9.40	d	+20.74	o	+39.62
F	-27.70	O	- 7.48	e	+23.43	p	+42.00
G	-25.90	P	- 6.41	f	+24.56	q	+44.71
H	-23.15	Q	- 4.70	g	+26.59	r	unresolved
I ₁	-20.95	R	- 3.35	h	+27.82		set of lines
I ₂	-20.28	S	- 1.35	i	+29.42	s	+51.26
I ₃	-19.11	T	+ 0.94	j	+30.84	t	+52.54
I ₄	-18.35						

actively stabilized. The reference laser was locked onto its emission line center, while the probe laser was sequentially locked onto each inverted Lamb dip which was strong enough to permit stabilization (the numbered lines in Figures 5.3 and 5.4. The resulting beat frequencies, as monitored on the spectrum analyzer, were reproducible to within 2 percent. Using the frequencies obtained for line 1 of P(18) and line 3 of P(16), the entire absorption spectra observed in our earlier experiment could be related to the laser line centers. Tables 5.1 and 5.2 show the resulting frequency assignments.

5.3 Discussion of Results

The technique of inverted Lamb dip absorption spectroscopy has been used to observe and measure the positions of 43 SF_6 absorption resonances coincident with the P(18) line and 24 resonances within the P(16) line of the 10.6μ band of the CO_2 laser. These line spacings, having separations on the order of 1 MHz, were measured and referred to the laser emission line center. This method has the advantage of resolution limited by the homogeneous linewidth (here > 1 MHz) rather than the inhomogeneous broadening, which for SF_6 is 29 MHz.

Classical infrared absorption spectra of SF₆ show strong absorption throughout the frequency range covered by the P branch of the CO₂ band around 10.6μ. It seems probable that a great many more absorption resonances can be found within the other P branch lines not examined here. These form an easily reproduced set of frequency markers of obvious use in CO₂ laser communications systems.

6. PLANS FOR NEXT SEMI-ANNUAL PERIOD.

The Stark modulation studies described in section 3 and the saturation studies described in section 5 will be continued. Additional gases will be investigated to see if they are suitable for use in Stark modulation schemes. In addition the questions of high frequency response and the possibility of F.M. modulation using the Pockel's effect in gases will also be investigated.

Two new efforts have been initiated and will be continued in the next six months. One of these efforts is aimed at developing our chemical laser capability so that we can investigate ways of modulating such radiation in the 2 ~ 5 micron wavelength region. The second effort is aimed at developing our PbSnTe technology so that we might use such material for photo detection and also as lasers in the 10 micron region. It is anticipated that such tunable PbSnTe lasers may be useful in our systematic search for gases suitable for the Stark modulation of CO₂ lasers.

7. REFERENCES

1. A. Landman and H. Marantz, 1969 Conference on Laser Engineering and Applications, Washington D.C., Paper 7.4.
2. P. C. Claspy and Yoh-Han Pao, Bulletin of the American Physical Society 14, 1193 (1969).
3. P. C. Claspy and Yoh-Han Pao, Journal of the Optical Society of America 60, 717 (1970).
4. P. H. Lee and M. L. Skolnick, Applied Physics Letters, 10, 303 (1967).
5. P. Rabinowitz, R. Keller, and J. T. LaTourette, Applied Physics Letters 14, 376 (1969).
6. I. Burak, J. I. Steinfeld, and D. G. Sutton, Journal of Applied Physics. 39, 4464 (1968).
7. Infrared and Raman Spectra, G. Herzberg, New York, D. Van Nostrand Co., 1945.
8. C. K. N. Patel and R. E. Slusher, Physical Review Letters 20, 1087 (1968).

8. LIST OF FIGURES

	<u>Page</u>
Figure 3.1 Experimental Apparatus for Stark Modulation	9
Figure 3.2 Stark Modulation	10
Figure 3.3 Typical Response During Simultaneous Modulation and Laser Sweep	13
Figure 3.4 Stark Modulation Response <u>vs.</u> AC Field Variation	19
Figure 3.5 Stark Modulation Response <u>vs.</u> DC Bias Variation	21
Figure 4.1 Apparatus for Laser Signature Experiments	25
Figure 4.2 Sequence of lines with 18 torr pressure and 11 ma discharge current	27
Figure 4.3 Sequence of lines with 17 torr pressure and 10 ma discharge current	27
Figure 4.4 Sequence of lines with 16 torr pressure and 10 ma discharge current.	28
Figure 4.5 Sequence of lines with 15 torr pressure and 8 ma discharge current. * Indicates lines of the 9.4 micron band	28
Figure 4.6 Sequence of lines with 14 torr pressure and 7.8 ma discharge current. * Indicates lines of the 9.4 micron band	29
Figure 4.7 Sequence of lines with 13 torr pressure and 6.8 ma discharge current. * Indicates lines of the 9.4 micron band.	29
Figure 4.8 Sequence of lines with 12 torr pressure and 6 ma discharge current.	30
Figure 4.9 Sequence of lines with 11 torr pressure and 5 ma discharge current.	30

	<u>Page</u>
Figure 4.10 Sequence of lines with 10 torr pressure and 4.4 ma discharge current	31
Figure 4.11 Sequence of lines with 15 torr pressure and 11 ma discharge current	31
Figure 4.12 Sequence of lines with 15 torr pressure and 10 ma discharge current.	32
Figure 4.13 Sequence of lines with 15 torr pressure and 9 ma discharge current. * Indicates lines of the 9.4 micron band.	32
Figure 4.14 Sequence of lines with 15 torr pressure and 8 ma discharge current. * Indicates lines of the 9.4 micron band.	33
Figure 4.15 Sequence of lines with 15 torr pressure and 7 ma discharge current. * Indicates lines of the 9.4 micron band.	33
Figure 4.16 Sequence of lines with 15 torr pressure and 6 ma discharge current.	34
Figure 4.17 Sequence of lines with 15 torr pressure and 5 ma discharge current.	34
Figure 4.18 Sequence of lines with 15 torr pressure and 10 ma current, cavity length L	35
Figure 4.19 Sequence of lines with 15 torr pressure and 10 ma current, cavity length increased to L + 100 microns.	35
Figure 4.20 Sequence of lines with 15 torr pressure and 10 ma current, cavity length increased to L + 200 microns.	36
Figure 4.21 Sequence of lines with 15 torr pressure and 10 ma current, cavity length decreased to L.	36

	<u>Page</u>
Figure 4.22 Sequence of lines with 15 torr pressure and 7 ma current	37
Figure 4.23 Sequence of lines with 15 torr pressure and 6 ma, fresh gas fill. * Indicates lines of the 9.4 micron band.	37
Figure 4.24 Sequence of lines with 15 torr pressure and 6 ma, polished NaCl flat in cavity . . .	38
Figure 4.25 Sequence of lines with 15 torr pressure and 6 ma, polished NaCl flat in cavity, small temperature gradient in NaCl. . . .	38
Figure 4.26 Sequence of lines with 15 torr pressure and 6 ma, polished NaCl flat in cavity, large temperature gradient in NaCl. . . .	39
Figure 4.27 Sequence of lines with 30 torr pressure and 10 ma current.	39
Figure 4.28 Sequence of lines with 25 torr pressure and 10 ma current.	40
Figure 5.1 Apparatus for Inverted Lamb Dip Absorption Spectroscopy.	44
Figure 5.2 Typical Absorption Spectrum.	45
Figure 5.3 SF ₆ Absorption Resonances Referred to the P(16) Line Center of CO ₂	47
Figure 5.4 SF ₆ Absorption Resonances Referred to the P(18) Line Center of CO ₂	48

9. LIST OF TABLES

	<u>Page</u>
Table 3.1 Molecular Gasses Suitable for Intracavity Stark Modulation of the Stronger CO ₂ Laser Lines	15
Table 5.1 Observed SF ₆ Absorption Line Centers Relative to the P(16) Line Center of CO ₂ . Line Designations are taken from Figure 5.3	49
Table 5.2 Observed SF ₆ Absorption Line Centers Relative to the P(18) Line Center of CO ₂ . Line Designations are taken from Figure 5.4..	50